A THESIS FOR THE DEGREE OF MASTER SCIENCE

Study on hydrodeoxygenation reaction of bio-oil in the presence of activated carbon supported Pd, Ru and Pt catalysts

활성탄에 담지된 팔라듐, 루테늄, 백금 촉매에 의한 바이오오일의
수첨탈산소 개질에 관한 연구

by Shinyoung Oh

PROGRAM IN ENVIRONMENTAL MATERIALS SCIENCE
GRADUATE SCHOOL
SEOUL NATIONAL UNIVERSITY
FEBRUARY, 2014

A THESIS FOR THE DEGREE OF MASTER SCIENCE

Study on hydrodeoxygenation reaction of bio-oil in the presence of activated carbon supported Pd, Ru and Pt catalysts

활성탄에 담지된 팔라듐, 루테늄, 백금 촉매에 의한 바이오오일의 수첨탈산소 개질에 관한 연구

by Shinyoung Oh

Advisor: Joon Weon Choi

PROGRAM IN ENVIRONMENTAL MATERIALS SCIENCE
GRADUATE SCHOOL
SEOUL NATIONAL UNIVERSITY
FEBRUARY, 2012

Study on hydrodeoxygenation reaction of bio-oil in the presence of activated carbon supported Pd, Ru and Pt catalysts

활성탄에 담지된 팔라듐, 루테늄, 백금 촉매에 의한 바이오오일의 수첨탈산소 개질에 관한 연구

지도교수 : 최 준 원

이 논문을 농학석사학위논문으로 제출함

2013년 11월

서울대학교 대학원
산림과학부 환경재료과학 전공
오 신 영

오신영의 석사학위논문을 인준함
2013년 12월

위 원 장 _____ (인)

부위원장 _____ (인)

위 원 _____ (인)

Abstract

Study on hydrodeoxygenation reaction of bio-oil in the presence of activated carbon supported Pd, Ru and Pt catalysts

Shinyoung Oh
Program in Environmental Material Science
Graduate School
Seoul National University

Miscanthus bio-oil was subjected to hydrodeoxygenation (HDO) with Pd/C, Ru/C and Pt/C at different temperatures (250, 300 and 350°C) and for different lengths of time (30, 45 and 60 min) in order to investigate chemical modification of micromolecules and macromolecules (lignin fragments) in bio-oil. Four main products – char, gas and two immiscible oils (heavy and light oil) – were obtained from the HDO reaction. Yields of heavy oil varied between 60.1 and 12.9% with Pd/C, 27.9 and 54.3% with Ru/C, and 56.3 and 34.9% with Pt/C. Yields of gas and char ranged from 6.5 to 35.6% and from 5.9 to 16.9%, respectively, in case of all catalysts. In terms of basic properties of heavy oil, water content decreased from 17.7 to 0.3-0.4% (Pd/C), 1.4-2.5% (Ru/C) and 1.3-3.9% (Pt/C) resulting in improvements in higher heating value (HHV) from 18.1 in bio-oil to 27.7-27.9 (Pd/C), 24.4-26.1 (Ru/C) and 21.0-24.0 (Pt/C) MJ/kg, respectively. Reduction of unstable oxygen-containing compounds such as acids (2-hydroxy-butanoic acid), aldehydes (furfural and vanillin) and sugars (levoglucosan) were confirmed by GC/MS analysis. Apart from hydrogenation and deoxygenation, micromolecules in bio-oil were

plausibly modified to stable esters and saturated components via demethoxylation, dealkylation, decarbonylation, dehydroxylation and ring opening.

Macromolecular lignin fragments (referred to as pyrolytic lignin (PL) in bio-oil and phenol polymer (PP) in heavy oil) were extracted and subjected to several types of analysis, such as elemental analysis, average molecular weight and of functional groups (OCH_3 and phen-OH), and the amount of ether linkages to investigate structural modification. Approximately 60% of PLs were decomposed to low molecular weight compounds. Moreover, OCH_3 and phen-OH groups attached to PL, decreased greatly from 11.6 and 6.8% to 0.1-1.7and 2.0-6.1%, respectively during the HDO reaction. The decrease in reactive functional groups indicates improved stability of bio-oil.

Catalysts were isolated from char and recycled three times to investigate catalyst reusability. With each cycle, catalysts were deactivated and the yield of heavy oil decreased to 52-60%, while char increased consistently by 2.9-4.5 times. Catalysts might be deactivated through various mechanisms, including coke deposition (Pd/C, Ru/C and Pt/C), slight destruction of active sites by metal-CH_3 formation (Pd/C).

Key words: Miscanthus, bio-oil, hydrodeoxygenation, pyrolytic lignin, phenol polymer, stability, noble metal catalyst

Student number: 2012-21118

Contents

List of Table

List of Figures

1. Introduction

1.1. Biofuel

As a result of growing environmental and economic concerns about fossil fuel, there is a high demand for renewable sources of energy; sources of concern about fossil fuels include their potential depletion, increases in oil prices and carbon dioxide emissions and consequent global warming. Estimates of future bioenergy availability range in 2050 ranged from 20 to 400 EJ, compared to a current global primary energy use of 465 EJ (Lysen, 2000). Many studies concerning carbon dioxide-neutral renewable energy have therefore been actively carried out across the world. Biomass is a promising renewable energy resource due to its absorption of CO_2 extracted from the atmosphere during growth. It can be converted into alternative carbon-based energy, especially as a liquid fuel which can be used in transportation to cater for high demand with low cost (Mohan et al., 2006). A wide range of biomass has potential to serve as a renewable energy resource, due to low sulfur, nitrogen and ash contents, which do not constitute an environment burden. Many types of biofuels, such as bio-oil, biodiesel, bioalcohol, biochar and syngas have therefore been produced from biomass by thermo-chemical and bio-chemical conversion processes (Bridgwater, 2012). While fossil fuels are used for electricity generation, industrial purposes and as transportation fuels, the latter is the most significant; two thirds of all energy is used for transportation purposes, with typically 63% of nonrenewable petroleum used for transportation energy in the US. The conversion of biomass to a liquid fuel for transportation might therefore result

in important advantages for environmental and economic strategies (Mohan et al., 2006).

As mentioned above, biomass can be converted to diverse bioenergy forms via biological and thermochemical processes. Well-known liquid transportation fuels are biodiesel and bioethanol from vegetable oils and cellulosic crops (Gray et al., 2006). Since these kinds of biomass are also edible, they can lead to an increase in food prices. Second-generation biomass, so-called lignocellulosic biomass and energy crop, is becoming prominent alternative sources of bioenergy (Wildschut et al., 2010b). The energy crop, Miscanthus is a perennial rhizomatous grass that has exhibited high water/nitrogen efficiency during its cultivation and could grow in a wide range of climatic and edaphic conditions. It also has potential for use in building materials or for bioremediation of contaminated soils. It is further able to serve as an either additional or alternative source of energy production due to its advantageous features including very low sulfur content, high calorific value, and low CO_2 balance which is very close to zero (Lysen, 2000).

1.2. Biomass to liquid (BTL) conversion

Currently available technologies for lignocellulosic conversion into liquid bioenergy include both biochemical- or thermochemical-based platforms (Huber et al., 2006). Biochemical conversion, often called the sugar platform, involves depolymerization of polysaccharides and fermentation of the resulting monosaccharides. Biochemical conversion of lignocellulosic biomass is harder than that of sugar-based biomass due to the complex structure of cellulose fibers embedded in a cross-linked lignin-hemicellulose matrix (Brown, 2003). A pretreatment process to improve the accessibility of cellulase on cellulose is necessary, in order for lignocellulosic biomass to be used for biochemical conversion. Subsequent processes are depolymerization of carbohydrates to sugars (hydrolysis) and fermentation of sugars to ethanol. The process of generating bioalcohol from starch and sugar bases is cost effective.

Thermochemical conversion is not as complicated process (Lee, 1997). It involves medium or high temperature degradation of biomass in an oxidized or reduced atmosphere to release inherent energy (combustion) or to produce fuel intermediates (energy carriers), such as synthesis gas (syngas) and pyrolysis liquids (Boateng et al., 2008). Since thermochemical conversion requires short reaction times and does not require pretreatment, it is considered to be a highly efficient technology, compared with biochemical conversion of lignocellulosic biomass.

Pyrolysis is a thermochemical conversion technology involving the thermal decomposition of an organic material in the absence of oxygen, leading to the formation of liquid, gases and a highly reactive carbonaceous char. Fast pyrolysis is a thermal decomposition process that occurs at

moderate temperatures with a high heat transfer rate to biomass particles and a short hot vapor residence time in the reaction zone (Czernik & Bridgwater, 2004). The process of fast pyrolysis is simple and yields of liquid products are high (50-75%). For these reasons, bio-oil from fast pyrolysis has become one of the most promising methods to convert renewable resources such as lignocellulosic biomass to liquid fuels and chemicals (Bridgewater, 2004).

1.3. Bio-oil upgrading technologies

Notwithstanding the benefits of fast pyrolysis, bio-oil is not suitable for direct application as a transportation fuel because of its high water (15-30%) and oxygen (35-40%) contents resulting in lower calorific value (17 MJ/Kg) (Bridgewater, 2004) compared to fossil fuel (40 MJ/kg). The viscosity and acidity of bio-oil are also relatively high and low thermal stability limits the direct use of bio-oil. Therefore, bio-oil needs reforming (division in physical or catalytic ways) of its undesired properties by reducing oxygen content.

Physical methods, such as hot-gas filtration, emulsification and solvent addition, offer a simple and inexpensive way to increase viscosity, especially in case of diesel. However, such physical upgrading technologies are unable to improve bio-oil to a suitable standard, regardless of their simplicity and inexpensiveness.

On the other hand, promising catalytic upgrading techniques such as hydrodeoxygenation (HDO), catalytic cracking of pyrolysis vapors and esterification, can improve bio-oil to an adequate standard for use as a transportation fuel. In detail, the process of catalytic cracking decomposes pyrolytic vapors to hydrocarbons by means of porous zeolite catalyst such as MCM-41, ZSM-5 an HZSM-5. In company with alcohol and catalyst, acids in bio-oil, which pose a problem of engine corrosion and most reactive compounds, are esterified. Hydrodeoxygenation, known as the most effective technology to obtain stable and high quality oil, also removes oxygen from oxygenated compounds in bio-oil as water or other compounds under high temperature and high pressure conditions using catalysts such as NiMo, CoMo, solid acid catalyst or noble metal catalyst with various supports (Ardiyanti et al., 2011; Czernik & Bridgwater, 2004; Qin et al., 2013).

1.4. Objectives

Bio-oil obtained from fast pyrolysis is unsuitable for combustion engines due to its undesirable properties, namely high water content, acidity, viscosity and oxygen level as well as low heating value. To overcome those problems, the upgrading of bio-oil has been studied. Among the upgrading technologies, HDO seems to produce higher quality oil with high yields.

Previous researches has mostly focused on HDO of model compounds, such as furfural and phenols; as lignin model compound (Ohta et al., 2011; Sitthisa & Resasco, 2011; Zhao et al., 2011). Since bio-oil is a mixture of various and complex compounds, the reactions of bio-oil during HDO might not be extrapolated from researches on the HDO of each model compounds. Moreover, the few studies conducted which deal with bio-oil focused on the effectiveness of catalysts on various supports (Wildschut et al., 2010b), and not on bio-oil properties. The main purpose of the experiment reported here was thus to improve the properties of bio-oil by HDO under supercritical conditions. Additionally the study sought to elucidate the effects of reaction temperature and time as well as of the kinds of metal supported on HDO catalysts. Palladium was chosen from among a number of noble metal catalyst for its high level of deoxygenation (Prochazkova et al., 2007). Ruthenium also showed a high level of deoxygenation (up to 90%), active for the hydrogenation of aromatic C-C bonds as well as producing high oil yield (up to 60%) (Wildschut et al., 2009). Platinum was reported to produce high catalytic activity for the production of hydrogen and was beneficial for the HDO of sorbitol and furan (Liu et al., 2012b). Activated carbon has advantages, as the optimum support material among three forms of carbon derived supports. Advantages include reduction of potential catalyst poisons

and pore plugging (Auer et al., 1998). Noble metals with activated carbon supports are presumed to be effective for HDO reactions. Catalyst loading and hydrogen pressure were fixed, based on previous research which investigated the influence of reaction temperature, time and type of noble metal catalyst, generally known as major factors affecting HDO. At the end of HDO, mass balances were constructed and essential physicochemical properties of the targeted liquid phase (heavy oil) were investigated. Despite large amounts and significant effects of pyrolytic lignin in bio-oil, there is no research concerning pyrolytic lignin in HDO oil. Therefore, macromolecules in bio-oil and heavy oil were analyzed to investigate changes in organic compounds in bio-oil during HDO.

2. Literature Review

2.1. Bio-oil production by fast pyrolysis

Fast pyrolysis process has been developed for bio-oil production since the oil crisis on the mid 1970s. Since then, several fast pyrolysis reactors have been developed with near-commercial status reached in the 1990s by Red Arrow Products Co., Inc., in Wisconsin, Dynamotive in Vancouver and BTG in the Netherlands (Czernik & Bridgwater, 2004). Fast pyrolysis is a simple and easy way to produce bio-oil by thermal decomposition under condition of moderate temperature (450-550°C) ambient pressure and very short reaction time (1-2 s) in the absence of oxygen. Chemical reaction kinetics, heat and mass transfer processes, as well as phase transition phenomena, therefore play important roles in fast pyrolysis. It can utilize whole biomass without pretreatment and produce high yields (ca. 50-75%) of bio-oil with 15-25% solid char and 10-20% non-condensable gases (Bridgewater, 2004). Lower process temperatures and longer vapor residence times favor the production of char, whereas high temperatures and long vapor residence times increase gas yields. Moderate temperatures and short vapor residence times are optimal for producing higher liquid yields .

2.2. Properties of bio-oil

Since bio-oil is formed by rapid and simultaneous depolymerizing and fragmenting of cellulose, hemicelluloses and lignin with a rapid temperature increase (Mohan et al., 2006), the properties of the products depend on reaction temperature, reaction time, heating rate, type of reactor as well as on feedstock. Bio-oil obtained through fast pyrolysis is a multi-component dark brown homogeneous mobile liquid (Meier et al., 2013). It can be used in burners, furnaces, boiler systems, diesels and gasoline engines and in turbines for electricity generation (Czernik & Bridgwater, 2004). Pyrolytic lignin (PL), which comprises approximately one fifth of bio-oil, has performed well as an adhesive or adhesive extender for waterproof plywood. Bio-oil, which is a mixture of various phenolic and carbohydrate derived compounds, can be converted into useful chemicals. However, separation techniques have not yet been developed on a larger scale due to the complexity of bio-oil (Czernik & Bridgwater, 2004).

2.2.1. Physicochemical properties of bio-oil

Generally, the 40% of oxygen content in bio-oil is present in identified compounds (Czernik & Bridgwater, 2004). Water content in bio-oil, which varies widely from 15-30%, results from the original moisture in the feedstock and from dehydration reactions occurring during pyrolysis (Oasmaa & Czernik, 1999). Therefore, the typical heating value of bio-oil is approximately 17 MJ/kg, which is similar to that of biomass and only 40-45% that of hydrocarbon fuels (40 MJ/kg). In general, viscosity of bio-oil ranges from 18.5-24.0 cSt at 40°C (Wildschut et al., 2009), depending on feedstock and experimental conditions and especially on the efficiency of collection of

low boiling components (Czernik & Bridgwater, 2004). Bio-oil obtained from biomass is also quite acidic in the range of pH 2-3.

2.2.2. Chemical composition of bio-oil

Even though there are differences depending on feedstock and pyrolysis conditions, bio-oil obtained from fast pyrolysis can be classified into four distinct fractions: 40% of medium-polar monomers detectable by GC, 12% of polar monomers detectable directly by HPLC or GC after derivatization, 28% of water derived from reaction water and feedstock moisture and 20% of oligomeric material, known as pyrolytic lignin (PL). PL, consisting of relatively small amounts of phenol, eugenol, cresols, and much larger quantities of alkylated phenols, is one of the major determinant factors of bio-oil properties, reactivity, and stability (Bayerbach & Meier, 2009).

Other influences of feedstock species are found in the lignin, from which the phenolics in bio-oils are primarily derived . Since oligomeric species in bio-oil are derived mainly from lignin but also from cellulose, bio-oil is a complex mixture of water, guaiacols, catechols, syringols, vanillins, furans, carboxaldehydes, isoeugenol, pyrones, acetic acid, formic acid and other carboxylic acids. It also contains other major groups of compounds, including hydroxyaldehydes, hydroxyketones, sugars, carboxylic acids and phenolics .

2.2.3. Disadvantages of bio-oil as a transportation fuel

Despite the advantages of a fast pyrolysis process, bio-oil has disadvantages as a transportation fuel, due to characteristics such as high viscosity, high water content and high acidity. Bio-oil is also complex mixture of organic compounds produced from thermal degradation of cellulose,

hemicellulose and lignin. High amount of unsaturated oxygen-containing compounds such as acida, aldehydes, alcohola and sugars are obtained from thermal decomposition (Torri et al., 2010). This results in low energy density, less than 50% that of conventional fuels and in immiscibility with hydrocarbon fuels. These characteristics make bio-oil unstable and preclude direct use of bio-oil as a transportation fuel. These disadvantages also resulted in engine corrosion, low mobility, fluidity, multiphase flow, clogging, high-pressure drops, and stoppage during provision of bio-oil to the vehicle engine (Czernik & Bridgwater, 2004).

2.3. Upgrading technologies

Bio-oil upgrading technologies can be roughly categorized into two kinds – physical and catalytical upgrading. Of the two, catalytic methods are known to be more effective (Bridgwater, 2012).

The representative physical upgrading method, emulsification, offeres a simple way to use bio-oil as a transportation fuel, by combining it with diesel. Although bio-oil is not miscible with hydrocarbons, it can be emulsified with diesel fuel with the aid of surfactants (Czernik & Bridgwater, 2004). The emulsion is more stable and has lower viscosity than bio-oil.

Catalytic cracking usually accomplishes deoxygenation through simultaneous dehydration, decarboxylation, and decarbonylation reactions occurring in the presence of zeolite catalysts. In the late 1970s, synthetic zeolites (e.g. ZSM-5) were successfully used to convert oxygenated organic compounds into hydrocarbons resulting in commercialization of the methanol-to-gasoline process. This discovery also stimulated research focused on the production of hydrocarbons from biomass-derived pyrolysis oil and pyrolysis vapors (Qin et al., 2013).

Esterification is a potential route to remove organic acids in bio-oil by reacting them with alcohol present in bio-oil or with added alcohol, resulting in improved of stability (Miao & Shanks, 2009).

HDO is one of the most effective hydrotreatment process which uses hydrogen to reduce the high oxygen content in bio-oil in the presence of suitable catalysts, such as sulfided cobalt-molybdenum or nickel-molybdenum (Ohta et al., 2011). This is known to be an effective bio-oil reforming process, which not only removes the oxygen in bio-oil, but also improves the stability of bio-oil by converting acids, aldehydes, alcohols and unsaturated compounds into more stable forms (Bridgwater, 2012).

2.4. Hydrodexoygenation (HDO)

Non-volatility and thermal instability of PL make bio-oil reforming a difficult process (Bayerbach & Meier, 2009). HDO with supercritical ethanol and suitable catalyst can convert PL into stable and noncorrosive organic compounds consisting of liquid phase (Tang et al., 2010). Generally, the HDO process starts at over 250°C, after stabilization of fragments and charring occurs under 250°C. HDO of phenol occurs at around 350°C, with catalyst and hydrogen pressure (Al-Sabawi & Chen, 2012). A suitable HDO catalyst needs to be able to effectively remove oxygen, suppress further decomposition and coke formation, and prevent deactivation. Though a homogeneous catalyst is more effective than a heterogeneous catalyst, the latter is preferred for the reasons of catalyst recovery. Generally and widely used sulfided metal catalysts, such as NiMo and CoMo, are problematic because the addition of sulfur to bio-oil results in fast deactivation of the catalyst by poisoning and contamination of water when the reactor is washed. Furthermore, liquid acid catalysts such as H_3PO_4 catalyze dehydration of cycloalkanol to cycloalkene. However, the recovery of catalyst from the reaction mixture is difficult (Ohta et al., 2011). Acids are also considered to be major reactive compounds, with consequent additional problems such as increasing instability and acidity. Thus, non-sulfided and acid-free catalysts, e.g. novel metal catalysts, bimetallic catalysts with activated carbon or aluminum-oxide supported catalysts, are now on researching and are producing effective results (Wildschut et al., 2010b). The use of noble metal catalyst is advantageous for HDO, because of highly active and stable characteristics with high hydrogenation properties. Noble metal catalysts are also less easily deactivated than more generally used metal sulfides .

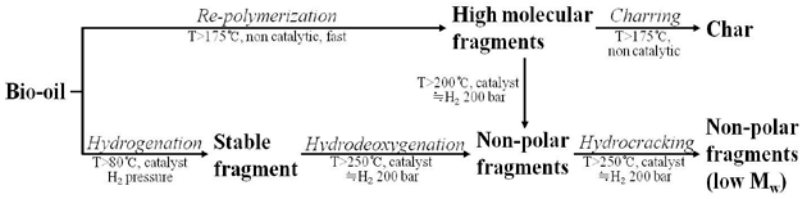

Figure 1. Proposed pathway for the hydrotreatment of bio-oil (Ardiyanti et al., 2011)

2.5. Catalyst deactivation

Deactivation of catalysts during the reaction is caused by various mechanisms and is hard to control. Typical contributions to catalytic deactivation include 1) the deposition of carbon as coke forms, 2) the blocking of active sites of catalysts (especially zeolite) by volatile components, 3) the competitive adsorption of reaction intermediates and 4) sintering and poisoning, resulting in loss of active phase (Bykova et al., 2013; Zhang et al., 2007). Deactivation levels and mechanisms usually depend on the support material as well as on the types of reaction catalyst used. For example, TiO_2, a generally used support material, sintered at 500°C in a hydrogen atmosphere, while Al_2O_3 is more resistant under the same conditions (Albers et al., 2001).

According to Auer et al., noble metals such as Pd, Ru and Pt performed well in hydrogenation. The Pd catalyst used olefin, aromatic ring and cyclohexene hydrogenation, reductive alkylation, C-O cleavage as well as conversion of carboxylic acid to alcohol. The Ru catalyst applied reactions such as aromatic ring hydrogenation and conversion of carboxylic acid to alcohol. The Pt catalyst often used olefin, cyclohexene and aromatic ring hydrogenation, reductive alkylation and C-O cleavage in the same way as the Pd catalyst (Auer et al., 1998). Previous studies have described how activated carbon can disperse and stabilize metallic particles, providing easy access of substances to the catalytic active phase (Auer et al., 1998).

3. Material and Methods

3.1. Materials

Miscanthus sinensis was used as the raw biomass to produce bio-oil by fast pyrolysis. Samples were ground to pass a 1 mm sieve, and then fed into the reactor which 1,000 g/hr fast pyrolysis system equipped with a fluidized-bed reactor. Fast pyrolysis was conducted under a nitrogen atmosphere at 500°C. The volatile pyrolytic products were passed through a cyclone, three coolers and an electrostatic precipitator, in which the product vapors were cooled and condensed to a liquid bio-oil with a yield of ca. 48.3 wt%. The detailed fast pyrolysis system was described in previous study (Bok et al., 2013).

Table 1. Fast pyrolysis experimental conditions

Sample	Name	*Miscanthus sinensis*
	Moist content (%)	1~2
	Amount of sample (g)	2000
	Particle size (mm)	1-2
Feeder	Feeding rate (g/min)	33.33
	Feeder RPM	400
	N_2 flow rate (L/min)	10
Reactor	Temperature (℃)	500
	Amount of sand(g)	5400
	N_2 flow rate (L/min)	50
Cooler	Temperature (℃)	10
Electrostatic precipitator	Current (mA)	0.5

3.2 Hydrodeoxygenation of bio-oil with noble metal catalysts

Bio-oil obtained from fast pyrolysis was hydrodeoxygenated in a 200 ml stainless steel (SUS316) autoclave reactor (900 mm height, 55 mm outer diameter and 2 mm wall thickness). The temperature of the reactor was controlled by an electric heating mantle combined with a cooling coil, passing through the water inside. The temperatures of the heating mantle and reactant were measured by thermocouple and thermometer, respectively. The device also included a mechanically driven stirrer, gas inlet and gas outlet. The reactor was filled with bio-oil and anhydrous ethanol (anhydrous grade, ≥ 99.5%) as a solvent (4:1, w/w) and 4 wt% of catalyst based on the weight of total reactant. Pd/C, Ru/C and Pt/C (Sigma Aldrich, 5 wt% active metal, on activated carbon) catalyst was used to compare HDO reaction mechanisms. The air inside the reactor was first flushed thoroughly with nitrogen gas and the pressure was raised to 30 bar with hydrogen gas. According to Ardiyanti et al., HDO initiates at over 250°C, with HDO of phenols occurring at around 350°C (Al-Sabawi & Chen, 2012; Ardiyanti et al., 2011; Gutierrez et al., 2009). The reactor was heated to the target reaction temperature (250, 300 or 350°C), with an average heating rate of 25°C/min and was maintained for 30, 45 or 60 min at each temperature. The reactor then cooled to 30°C, with an average cooling rate of 10°C/min after the end of reaction. Stirring of the reactant was started at 350 rpm with a mechanical turbine-type stirrer. The three phases of reaction products were liquid, char and gas. The liquid product, consisting of an upper water-rich phase (light oil) and lower organic phase (heavy oil) was recovered from the reactor and separated using a separatory funnel. Subsequently, the reactor was rinsed with anhydrous ethanol. Finally,

ethanol fractions with the organic phase and suspended solids were filtered. After filtration, the filter was placed at ambient temperature to dry off, and then weighed to obtain the yield of char. The filtrate was evaporated at 30°C for recovery of the organic phase. At each step, experiments were conducted in duplicate. Experiments started under mildest conditions of 250°C and 30 min, allowing for increased reaction time and temperature. Heavy oil was named after HDO catalyst, as Pd1 to Pd9, Ru1 to Ru9 and Pt1 to Pt9, respectively. Overall experimental process was described in Fig. 3. All experiments were accomplished in duplicate. The yield of char, light oil and heavy oil were calculated by the following equation.

$$\text{Yield of char (\%)} = [\text{Solid (g)} - \text{Catalyst (g)}] / [\text{Bio-oil (g)} + \text{Solvent (g)}] \times 100$$

$$\text{Yield of light oil (\%)} = [\text{Light oil (g)}] / [\text{Bio-oil (g)} + \text{Solvent (g)}] \times 100$$

$$\text{Yield of heavy oil (\%)} = [\text{Heavy oil (g)}] / [\text{Bio-oil (g)} + \text{Solvent (g)}] \times 100$$

$$\text{Yield of gas (\%)} = 100 - [\text{yield of light oil} + \text{yield of heavy oil} + \text{yield of char}]$$

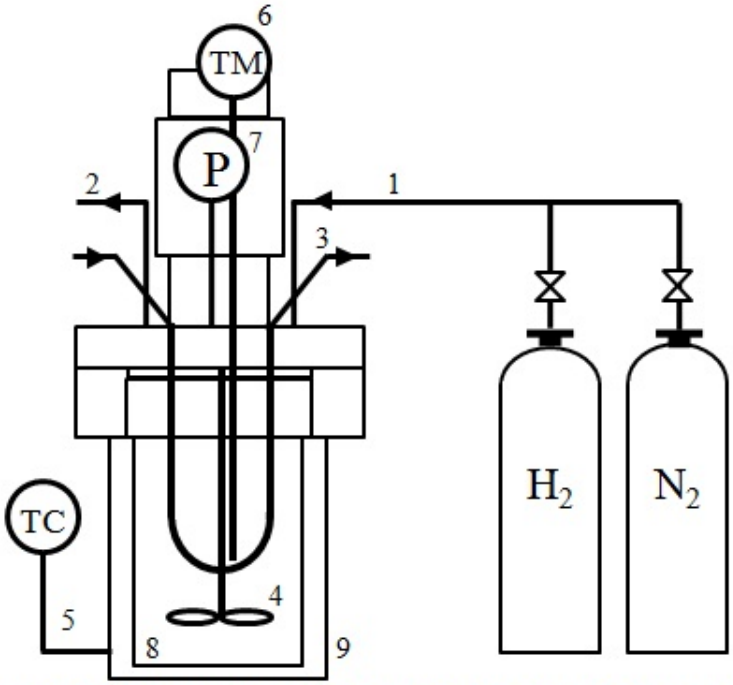

1: gas inlet, 2: gas outlet, 3: cooling coil, 4: stirrer, 5: thermocouple
6: thermometer, 7: pressure gage, 8: liner, 9: heating mantle

Figure 2. Scheme of hydrodeoxygenation reactor

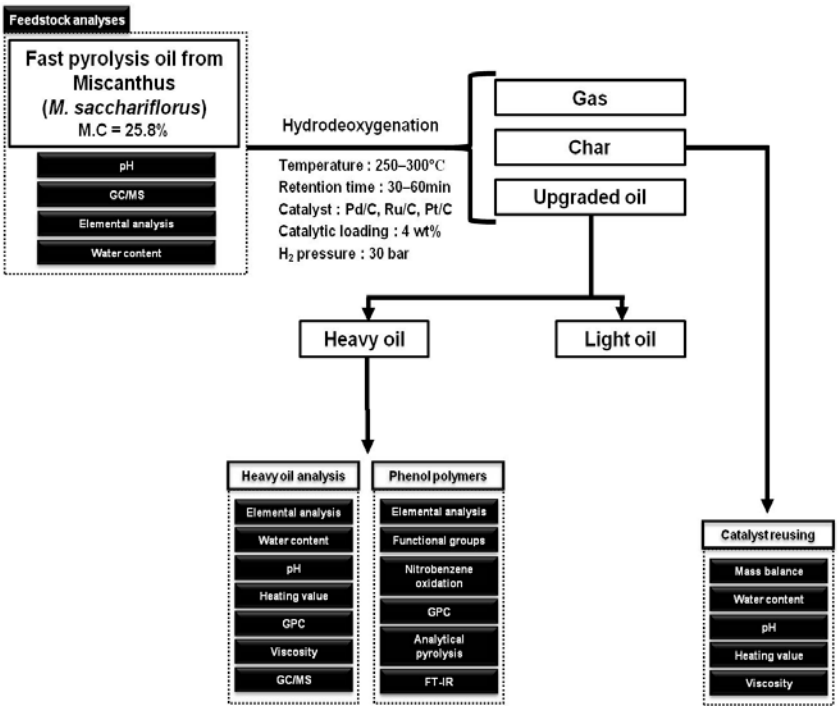

Figure 3. Illustration of the overall experimental and analysis method of different hydrodeoxygentation conditions

3.3 Characterization of heavy oil

3.3.1. Physicochemical properties

Karl-Fischer titration (Titro line KF, Schott, Germany) with hydranal composite 5 solution was used to measure the water content of bio-oil and heavy oils. After calibration with standards (5mg water/ml MERCK 1.09259 250) and distilled water, the water content of samples was measured. 100-200mg of sample were injected into the dried-methanol solvent and the water was titrated using a titration reagent. pH was measured using a pH meter (Thermo Fisher Scientific Inc., USA). Viscosity was determined by capillary-type viscometer and ViscoClock (Schott, Germany) at 40°C. The average molecular weights of control and heavy oils were measured using a GPC max instrument (Viscotek RImax, Viscotek, UK) coupled with a UV-Vis detector (VE3210, Viscotek). UV-Vis detector was equipped with PLgel 5 μm MIXED-C columns (300 × 7.5 mm, Varian, Inc.) and PLgel 5 μm guard columns (50 × 7.5 mm, Varian, Inc.). Each 2mg sample was dissolved in 2ml tetrahydrofuran (THF) and filtered using 0.5μm pore size hydrophobic syringe filter to remove insoluble solids. Polystyrene with mass ranges between 580 Da and 3,250 kDa was used as a standard to create a calibration curve.

Elemental analysis for carbon, hydrogen, and nitrogen was carried out with a LECO CHNS-932 analyzer. In this analysis, carbon, hydrogen and nitrogen were simultaneously determined as gaseous products (carbon dioxide, water vapor and nitrogen). The oxygen content was calculated by difference (100% - C% - H% - N%). Higher heating value (HHV) was calculated by Sheng and Azvedo's formula (Sheng & Azevedo, 2005) and are presented in Table 2.

3.3.2. Qualification of low molecular compounds (micromolecules) in heavy oil

For qualitative analysis of micromolecules in bio-oil and heavy oils, GC/MS was used. Fluoranthene was used as an internal standard (50 μl of 25 mg/ml acetone) and added to 450μl of each oil. Separation of micromolecules in oils was conducted with a split ratio of 1:20. Agilent 7890A, coupled with a 5975C mass selective detector and a flame ionization detector equipped with DB-5 capillary column (60 m x 0.25 mm x 0.25 μm). The oven temperature was maintained at 50°C for 5 min, followed by a heating rate of 3°C/min to 280°C, with this temperature maintained for 20 min. Injector and FID detector temperatures were 250°C and 300°C, respectively. Each peak was identified by comparison to NIST (National Institute of Standards and Technology) mass spectra data library and previous researches (Faix et al., 1991; Faix et al., 1990).

3.4. Macromolecular lignin fragments from heavy oil

3.4.1. Extraction of lignin fragments

The macromolecular lignin fragment (macromolecules, in briefly) was extracted from bio-oil heavy oil by the method described by Scholze and Meier (Scholze & Meier, 2001). As similar yield of macromolecules was collected from bio-oil and bio-oil/ethanol mixtures, macromolecules were extracted from the bio-oil/ethanol mixture, due to the sticky appearance from bio-oil. Each 4 g of heavy oil and bio-oil were dissolved in 10 ml of ethanol. Subsequently, a homogenized, mixed solution was added into 150 ml of ice-cooled water in drops, with stirring over 24 h. After separation of the water-insoluble phase by centrifugation, this was re-diffused for 4 h to completely remove the water-soluble fraction. After separation and freeze-drying, powder form solid fractions (macromolecules) were obtained. Macromolecules extracted from bio-oil were labeled as ‘pyrolytic lignin (PL)’ while those from heavy oil were labeled as ‘phenol polymer (PP)’, followed by the name of the noble metal, for example Pd PP1.

3.4.2. Functional groups and elemental analysis of macromolecules

Elemental analysis was conducted according to same method as mentioned above. Essential functional groups (phen-OH and OCH_3) of macromolecules were determined according to the method by Baker (Baker, 1996) and Mansson (Månsson, 1983), respectively. Nitrobenzene oxidation was performed by method of Iiyama and Lam (Iiyama & Lam, 2006).

3.4.3. Gel permeation chromatography

The average molecular weights of biooil and heavy oils were measured using a GPC max instrument (Viscotek RImax, Viscotek, UK) coupled with a UV-Vis detector (VE3210, Viscotek). UV-Vis detector was equipped with PLgel 5 μm MIXED-C columns (300×7.5 mm, Varian.) and PLgel 5 μm guard columns (50×7.5 mm, Varian.). Mass range between 580 Da and 3,250 kDa polystyrene was used as standards to create a calibration curve.

3.4.4. Thermanalytical and spectroscopic analysis of macromolecules

A pyroprobe (Pyroprobe 2000, CDS Analytical.) was used for analytical pyrolysis. Each sample (0.8±0.05 mg) with 1 μL internal standard (1.25 mg of fluoranthene/ml of methanol) was loaded into a quartz cup with glass wool and pyrolyzed isothermally at 600°C for 20 s. Released volatile products were transferred via gas chromatographer (Agilent 7890A) equipped with a DB-5ms column (60 m x 250 μm x 0.25 μm) with a split ratio of 1:200. The oven temperature was initially 50°C and was maintained for 1 min, followed by heating at a rate of 3°C/min to 130°C, 1.5°C/min to 180°C, and then 6°C/min to 280°C, with this temperature maintained for 5 min. Injector and detector temperatures were 320°C and 300°C, respectively. Each peak was identified by comparison to the NIST MS Search 2.0 mass spectra data library and previous research (Faix et al., 1991; Faix et al., 1990). FT-IR spectra were recorded on a Nicolet 6700 spectrometer (Thermo Scientific, USA) operating 32 times in the wavelength range of 4000–650 cm^{-1} with a resolution of 8 cm^{-1}.

3.5. Reuse of HDO catalysts

To investigate the reusability of each noble metal catalyst, catalyst separation was conducted based on the method of Zhao et al. (Zhao et al., 2011). At the end of the HDO reaction, the solid phase, a mixture of char and catalyst, was isolated from the liquid (light oil and heavy oil). Since char exists both as a deposited on the catalyst as well as in powder form with low density, causing catalyst deactivation by blocking of the active site (Fahmi et al., 2007), a two-step reaction was needed to separate catalyst and char. First, to remove the low density char, the mixture was decanted with water. This was then washed with ethyl acetate, to remove char deposited on the catalyst or tar-like char. After 24h of freeze-drying, the catalyst was reused for a subsequent HDO reaction without any further treatment. Catalysts were used in their fresh state, then recycle three times. Heavy oil obtained from recycled catalyst was labeled on the basis of the catalyst used and the number of catalyst recycling cycle, for example, Pd-1st, Pd-2nd and Pd-3rd.

4. Results and Discussion

4.1. Bio-oil modifications during HDO with Pd/C catalyst

4.1.1. Mass balance of hydrodeoxygenation products

4.1.1.1. Influence of reaction temperature

The HDO reaction was performed at 250, 300 and 350°C to investigate the effect of reaction temperature on the HDO of bio-oil. At these conditions, four kinds of products (gas, char and two immiscible liquids, heavy oil and light oil) were obtained as HDO products. A target product in this study, heavy oil, had a black, sticky and oily flavor organic phase, whereas light oil had an oxygen-rich (75.4-80.4%) transparent brown water phase. Yield of each product was based on the weight of bio-oil as function of temperature as presented in Table 1.

The yield of each product revealed that the composition of HDO products was considerably affected by temperature. As shown in Table 1, the yield of heavy oils (Pd1-9) ranged between 12.9-60.1% based on the weight of bio-oil. Also, the yield of heavy oils gradually decreased with increasing reaction temperature, from 60.1-31.3% (30 min), from 51.5 to 16.5% (45 min) and from 46.3 to 12.9% (60 min). Light oil yield was similar at 30 min: from 23.5 to 31.8%; at 45 min: from 33.7 to 41.1%; at 60 min from 31.8 to 38.0% compared with heavy oils. At a reaction time of 60 min, the yield of gas slightly increased up to 300°C (16.8%) and then drastically increased at 350°C (32.2%). This trend resulted from further decomposition of organic compounds in the liquid phase (light oil and heavy oil) (Joshi & Lawal, 2012). Concurrently, the yield of char contemporaneously increased from 6.2 to 16.9%

with increasing reaction temperature. These results indicate that polymerization and further decomposition which lead to an increase in gas and char yields were also accelerated by increasing reaction temperature.

4.1.1.2. Influence of reaction time

Because reaction time is another major factor that determines product yield, reaction time was controlled (30, 45 and 60 min) at 250, 300 and 350°C, respectively. The yields of the four main products based on the weight of the bio-oil are shown in Table 1. The yield of heavy oils steadily decreased from 60.1 to 46.3% (250°C), from 48.9 to 37.4% (300°C) and from 31.3 to 12.9% (350°C) with increasing reaction time, while that of gas and char increased with increasing reaction time. These results are consistent with the previous study, and this might be due to polymerization and further decomposition that were predominantly enhanced with increasing reaction time (Wildschut et al., 2010a). Therefore, heavy oil drastically decreased from 31.3 to 12.9% and gas yield increased from 19.2 to 35.6% at 350°C. This suggests that long reaction time as well as high reaction temperature induced further decomposition of organics into gas rather than conversion of bio-oil into heavy oil.

Table 2. The distribution of product yields as a function of reaction temperature and reaction time (wet basis, Pd/C catalyst loading: 4wt%, H_2 pressure: 30 bar)

Yield (%)	Pd1	Pd2	Pd3	Pd4	Pd5	Pd6	Pd7	Pd8	Pd9
	250°C 30min	250°C 45min	250°C 60min	300°C 30min	300°C 45min	300°C 60min	350°C 30min	350°C 45min	350°C 60min
Char	5.9 (0.3)[a]	9.4 (0.9)	6.2 (2.3)	8.9 (2.4)	5.5 (1.1)	10.4 (2.1)	15.7 (2.7)	16.1 (0.8)	16.9 (2.2)
Light oil	23.5 (1.6)	31.8 (1.5)	31.7 (0.8)	33.7 (1.8)	41.1 (0.3)	35.4 (2.8)	33.8 (5.1)	31.8 (0.5)	38.0 (7.4)
Heavy oil	60.1 (0.5)	51.5 (1.5)	46.3 (1.8)	48.9 (2.1)	41.6 (1.4)	37.4 (1.3)	31.3 (1.1)	16.5 (4.4)	12.9 (5.5)
Gas	10.5 (1.8)	7.4 (0.8)	15.8 (1.4)	8.5 (2.7)	11.7 (0.0)	16.8 (3.7)	19.2 (1.3)	35.6 (4.1)	32.2 (4.1)

[a]: Standard deviation

4.1.2. Characterization of heavy oil

4.1.2.1. Physicochemical properties

Generally, hydrogenation and deoxygenation during HDO could improve bio-oil properties such as heating value and thermal stability (Joshi & Lawal, 2012). Therefore, several physicochemical properties such as water content, pH and viscosity were determined and the results are presented in Table 2. The water content related to heating value and combustion properties in the engine decreased from 17.7% in bio-oil to 0.1-0.8% in heavy oils during the HDO reaction. No clear relationship between water content and reaction time existed. Water content slightly decreased with increasing reaction temperature, especially from 0.8 (250°C) to 0.1% (350°C) at 60 min. This tendency was elucidated by the dehydration of the organic phase improved with increasing reaction temperature (Wildschut et al., 2010a). The pH value of bio-oil (2.5) increased to 4.0-5.0 in heavy oil, with no significant differences between conditions. From these results, it could be expected that acids derived from the decomposition of carbohydrates might be shifted into desired compounds like esters and ketones. This hypothesis will be described in depth in the following sections.

Previous studies reported that the viscosity of bio-oil ranged from 18.5-24.0 cSt and heavy oil ranged from 6.1-7.3 cSt at 40°C due to supercritical ethanol reacting as a partial solvent with bio-oil (Oasmaa et al., 2004; Wildschut et al., 2009). Because the high viscosity of bio-oil resulted in many disadvantages during injection into a vehicle engine (Martínez-Palou et al., 2011), reducing viscosity is an important point of reforming bio-oil into transportation fuel. In this experiment, viscosity decreased from 29.6 cSt for bio-oil to 2.8-6.4 cSt for heavy oil, similar to previous studies.

HDO leads to decreased oxygen levels in bio-oil due to deoxygenation, which could be crucial for value-added utilization of bio-oil since high

oxygen levels result in high acidity and low heating value. Elemental composition and higher heating value were determined and these results are presented in Table 2. A Van Krevelen diagram is also provided to describe the molar O/C and H/C ratio of bio-oil and heavy oil corresponding to each reaction condition (Fig. 2). As shown in Table 2, 40 wt% of carbon content in bio-oil increased to 51.5-63.3 wt% in heavy oils while oxygen content decreased from 52.2 wt% in bio-oil to 27.2-38.5 wt% in heavy oils. Especially heavy oils 8 and 9 (350°C at 45 and 60 min) showed relatively high carbon levels, 61.2-63.3 wt%, and low oxygen levels, 27.2-28.9 wt%, compared with those of heavy oil, 1-6. These results were caused by removal of oxygenated compounds in bio-oil to gas or light oil phase at high temperature, as shown in section 3.3. Removal of oxygenated compounds also resulted in higher HHV of heavy oils 8 and 9 (25.4-25.9 MJ/kg) compared with bio-oil (17.3 MJ/kg) and other heavy oils (22.8-24.2 MJ/kg). This indicates that deoxygenation became predominant with increasing reaction temperature (heavy oil 8 and 9). Fogassy et al. (Fogassy et al., 2011) referred to a promising elemental composition of heavy oil that we named ‘ideal heavy oil’ in this study. It is plotted in Fig. 2. After the HDO, the O/C ratio of bio-oil (1.0) decreased to 0.3-0.6 due to deoxygenation. The H/C ratio of bio-oil (2.2) also decreased to 1.8-2.2. All heavy oils showed a well-deoxygenated state compared with bio-oil. The O/C ratio of heavy oil 8 was 0.3, which was the most similar value to ideal heavy oil. However, those values needed to be improved on to reach the ideal O/C ratio (0.02).

Table 3. Physicochemical properties of bio-oil and heavy oils (wet basis, Pd/C catalyst loading: 4wt%, H_2 pressure: 30bar)

	Biooil	Pd1	Pd2	Pd3	Pd4	Pd5	Pd6	Pd7	Pd8	Pd9
Water content(wt%)	17.7	0.2	0.4	0.8	0.4	0.3	0.4	0.1	0.2	0.1
pH	2.5	4.7	4.0	4.5	4.9	5.0	4.7	5.0	4.9	5.0
Viscosity(cSt)[a]	29.6	3.7	6.4	5.8	2.8	2.4	5.4	3.6	4.1	3.7
C (wt%)	40.0	57.1	51.5	55.6	55.3	54.5	58.1	56.2	63.3	61.2
H (wt%)	7.5	8.9	9.7	9.0	10.0	10.1	9.0	8.9	9.3	9.5
N (wt%)	0.2	0.2	0.1	0.1	0.1	0.0	0.1	0.1	0.1	0.2
O[b] (wt%)	52.2	33.6	38.5	35.2	34.5	35.3	32.7	34.7	27.2	28.9
S (wt%)	0.2	0.2	0.2	0.1	0.1	0.1	0.1	0.1	0.1	0.2
HHV(MJ/kg)[c]	17.3	23.9	22.8	23.5	24.1	23.9	24.2	23.6	25.9	25.4

[a]:Measured at 40°C
[b]:Calculated by difference
[c]:High heating value was calculated following formula (Sheng & Azevedo, 2005),
HHV(MJ/kg) = -1.3675 + (0.3137 X C) + (0.7009 X H) + (0.0318 X O)

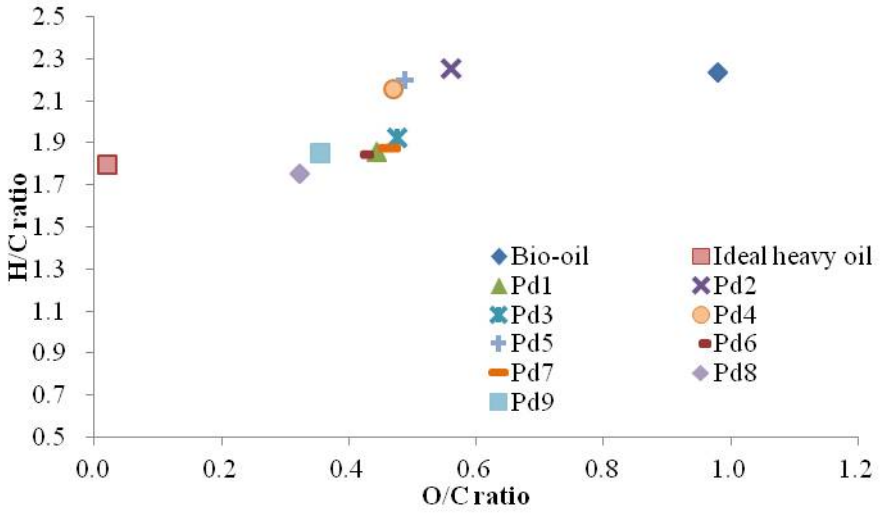

Figure 4. Van Krevelen diagram of bio-oil, heavy oils performed with Pd/C

4.1.2.2. Qualification of low molecular compounds and plausible modifications

During fast pyrolysis, lignocellulosic biomass components (cellulose, hemicellulose and lignin) suffer from various thermochemical degradation reactions (cracking, dehydration, decarbonylation, and ring opening etc.) (Furimsky, 2000; Sitthisa & Resasco, 2011). Therefore, bio-oil is considered a complicated mixture of various chemicals such as water, volatile low molecular weight compounds, polar high molecular weight compounds and lignin fragments, in which volatile low molecular weight compounds are referred to as ‘micromolecules’ and lignin fragments as ‘macromolecules’ in this study.

A total of 32 kinds micromolecules in oils were identified from GC/MS analysis and heavy oils mainly consisted of various monomeric phenols such as guaiacol, 4-ethyl-phenol and 4-propyl-phenol. Micromolecules were classified based on their chemical structure and kinds of functional groups. The distribution of the relative concentration of classified compounds in heavy oils is displayed in Fig. 3. As shown in Fig. 3, common changes occurred such as decreases in acids, aldehydes, sugars and alkylbenzenes and increasing esters during the reaction. Notably, heavy oils 4-6 had a small amount of alkylbenzenes and an increased amount of ketones compared with bio-oil. Moreover, heavy oils 7-9 revealed low micromolecule concentrations compared with heavy oils 4-6 because of their further decomposition during HDO. A similar trend was observed in heavy oils 1-3, but it might be due to an incomplete reaction at the starting temperature (250°C) of HDO (Gutierrez et al., 2009).

In Table 3, detailed micromolecules in the Pd1-9 are listed. The values are expressed as an area ratio between micromolecules in oils and a certain amount of internal standard added before GC/MS analysis. Those in parentheses indicated the plausible portion of each compound in oil. Pd5 and Pd6 showed a 27.6% increase and 52.8% decrease in micromolecules compared with bio-oil, respectively, which indicates that HDO might be dominant after polymerization and further decomposition may occur with increasing reaction time. Phenols were increased from 31.4% in bio-oil to 73.9-76.1% in heavy oils. Typically unsaturated 4-vinyl-phenol (2.4%) and 4-(1-propenyl)-guaiacol (1.6%) in bio-oil decreased while 4-ethyl-phenol (15.5-17.7%), 4-methyl-guaiacol (8.3-8.6%) and 4-propyl-guaiacol (6.9-8.3%) increased in heavy oils. Moreover, phenol, not detected in bio-oil, was 3.1-3.4% of the final product after HDO via demethoxylation, demethylation and hydrogenation. Evidently, unstable and undesired compounds such as 2-hydroxy-butanoic acid, furfural, levoglucosan and butandial in bio-oil were clearly removed and relatively stable esters such as 4-oxo-pentanoic acid ethyl ester, hexadecanoic acid ethyl ester and octadecanoic acid ethyl ester in heavy oil increased. It was due to hydrogenation, decarbonylation, dehydroxylation and ring opening. Though aldehydes and acids causing acrid and pungent odor were removed, the lingering odor might be an inherent property of miscanthus bio-oil that originates from non-detectable low molecular compounds (Lee et al., 2010).

Based on GC/MS analysis, it is possible that phenol derivatives having vinyl/oxygenated functional groups might be converted into stable phenol compounds, and that other unstable functional groups also changed. Therefore, plausible chemical modifications such as demethoxylation, hydrogenation, dealkylation, ring opening, decarbonylation and dehydroxylation based on the

amount of micromolecules are presented in Table 4. The 3.1-3.4% of phenol produced after HDO could be derived from demethoxylation of guaiacol and syringol (Bui et al., 2011). Regardless of demethoxylation to phenol, guaiacol (7.3%) and syringol (1.6%) in bio-oil increased 14.6-15.5% and 6.9-8.3% in heavy oils, respectively. This was due to dealkylation via hydrogenation (Furimsky et al., 1986) and it was confirmed by elimination of 4-methyl-syringol (0.8%) and 4-(1-propenyl)-guaiacol (1.6%) in bio-oil. Meanwhile, 2-methyl-benzofuran (4.1%) in bio-oil was eliminated and 2-methyl-phenol (3.2-3.8%) was formed in heavy oils. It could be elucidated by dealkylation via ring opening (Furimsky, 2000; Liu et al., 2012b). Considering that 2-propyl-phenol as an intermediate of the above reaction remained more concentrated in heavy oil (1.7-10.8%) than in bio-oil (2.4%), ring opening of furan progressed further compared with the dealkylation of 2-methyl-phenol. In a previous study, deformation of a phenolic hydroxyl and an aromatic ring was hard to observe compared with ring opening of furfural and levoglucosan (Al-Sabawi & Chen, 2012). Thus, formation of esters, which are produced by hydrogenation, dehydroxylation and decarbonylation during the HDO of bio-oil, could be derived from furfural and levoglucosan, but not from an aromatic ring (Sitthisa & Resasco, 2011). Through the above-mentioned chemical modification routes, micromolecules in bio-oil were converted into further stable forms in heavy oils.

Table 4. Quantitative analysis of low molecular weight components in bio-oil and heavy oil (wet basis, Pd/C catalyst loading: 4wt%, H_2 pressure: 30bar)

	Compound	Relative area(peak area/ I.S. area)									
		Bio-oil	Pd1	Pd2	Pd3	Pd4	Pd5	Pd6	Pd7	Pd8	Pd9
	Acids										
1	Butanoic acid, 2-hydroxy-	0.5 (4.5)	-	-	-	-	-	-	-	-	-
	Phenols										
2	Phenol	-	0.6 (4.7)	0.9 (4.9)	0.9 (6.7)	0.4 (3.1)	0.5 (3.2)	0.2 (3.5)	2.8 (9.8)	2.8 (10.6)	2.4 (9.6)
3	2-Methyl-phenol	-	0.8 (6.1)	1.0 (5.3)	0.7 (5.3)	0.5 (3.8)	0.5 (3.2)	0.2 (3.5)	1.6 (5.5)	1.3 (4.9)	1.3 (5.3)
4	4-Methyl-phenol	-	1.8 (13.2)	1.9 (10.5)	1.3 (10.5)	0.3 (2.3)	0.5 (3.2)	0.2 (3.5)	3.5 (12.2)	2.9 (10.8)	2.9 (11.5)
5	Guaiacol	0.9 (8.1)	1.7 (12.5)	1.9 (10.5)	1.3 (10.5)	1.9 (14.6)	2.1 (15.6)	0.9 (15.8)	2.9 (10.1)	2.7 (10.0)	2.3 (9.0)
6	2,4-Dimethyl-phenol	-	0.2 (1.1)	0.2 (1.0)	0.3 (2.1)	0.1 (0.8)	0.1 (0.6)	-	1.9 (6.8)	1.0 (3.7)	1.0 (4.1)
7	4-Ethyl-phenol	0.3 (2.7)	1.9 (13.8)	2.8 (15.4)	2.1 (16.8)	2.3 (17.7)	2.6 (16.9)	0.9 (15.8)	4.9 (17.5)	4.9 (18.2)	4.8 (18.9)
8	2,3-Dimethyl-phenol	0.3 (2.7)	-	-	-	-	-	-	-	-	-
9	4-Methyl-guaiacol	0.3 (2.7)	0.8 (6.1)	1.1 (6.2)	0.9 (7.1)	1.1 (8.5)	1.3 (8.4)	0.5 (8.8)	2.0 (6.9)	2.6 (9.7)	2.1 (8.5)
10	4-Vinyl-phenol	0.3 (2.7)	-	-	-	-	-	-	-	-	-
11	2-Propyl-phenol	0.3 (2.7)	0.4 (3.1)	0.6 (3.2)	0.4 (3.0)	0.3 (2.3)	1.7 (11.0)	0.1 (1.8)	0.9 (3.2)	0.7 (2.8)	0.6 (2.3)
12	4-Ethyl-guaiacol	0.2 (1.8)	1.6 (11.8)	2.0 (10.8)	1.3 (10.2)	1.5 (11.5)	-	0.6 (10.5)	2.2 (7.9)	2.3 (8.7)	2.6 (10.3)
13	Syringol	0.2 (1.8)	1.0 (7.2)	1.6 (8.8)	0.9 (7.0)	0.6 (4.6)	0.7 (4.5)	0.3 (5.3)	1.2 (4.1)	1.0 (3.8)	0.9 (3.4)
14	4-Propyl-guaiacol	0.6 (5.4)	0.9 (6.9)	1.3 (7.4)	0.9 (7.0)	0.9 (6.9)	1.3 (8.4)	0.4 (7.0)	1.6 (5.7)	1.6 (5.8)	1.4 (5.4)
15	4-Methyl-syringol	0.1 (0.9)	-	-	-	-	-	-	-	-	-
16	4-(1-Propenyl)-guaiacol	0.2 (1.8)	-	-	-	-	-	-	-	-	-
	Aldehydes										
17	Furfural	1.3 (11.7)	-	-	-	-	-	-	-	-	-
	Sugars										
18	Levoglucosan	2.1 (18.9)	-	-	-	-	-	-	-	-	-
	Esters										
19	Pentanoic acid, 4-oxo-, ethyl ester	-	1.1 (8.4)	1.1 (06.0)	0.7 (5.6)	0.4 (3.1)	0.5 (3.2)	0.2 (3.5)	1.1 (3.9)	1.0 (3.8)	1.0 (3.7)
20	Hexadecanoic acid, ethyl ester	-	-	-	-	0.3 (2.3)	0.3 (1.9)	0.1 (1.8)	0.1 (0.3)	0.1 (0.4)	0.1 (0.4)
21	Octadecanoic acid, ethyl ester	-	-	0.1 (0.7)	0.1 (0.9)	0.1 (0.8)	0.1 (0.6)	-	0.1 (0.3)	0.1 (0.4)	0.2 (0.7)
	Alcohols										
22	Butanedial	0.2 (1.8)	-	-	-	-	-	-	-	-	-
	Ketone										
23	2-Methyl-cyclopentanone	-	-	0.5 (2.8)	0.4 (2.9)	0.2 (1.5)	0.1 (0.6)	0.1 (1.8)	0.2 (0.7)	0.3 (1.1)	0.4 (1.6)
24	2-Ethyl-cyclopentanone	-	-	-	0.2 (1.7)	0.8 (6.2)	0.9 (5.8)	0.3 (5.3)	0.2 (0.7)	0.2 (0.7)	0.3 (1.0)
25	2,5-Hexanedione	-	-	0.5 (2.8)	-	0.1 (0.8)	0.2 (1.3)	0.1 (1.8)	-	-	-
26	2-Ethyl-2-cyclopentenone	0.4 (3.6)	0.3 (2.3)	0.2 (1.3)	-	-	0.1 (0.6)	-	0.1 (0.3)	0.1 (0.4)	0.1 (0.4)
27	2,3-Dimethyl-2-cyclopentenone	0.4 (3.6)	0.4 (2.6)	0.5 (2.5)	0.4 (2.9)	0.9 (6.9)	1.2 (7.8)	0.5 (8.8)	1.1 (3.9)	1.1 (4.2)	1.0 (4.1)
28	4-Hydroxy-5,6-dihydro-(2H)-pyranone	0.3 (2.7)	-	-	-	-	-	-	-	-	-
29	2-Hydroxy-3-methyl-2-cyclopentenone	0.4 (3.6)	-	-	-	-	-	-	-	-	-
	Alkylbenzenes										
30	1,3-Dimethyl- benzene	1.3 (11.7)	-	-	-	-	-	-	-	-	-
31	1,2,3-trimethoxy-5-methyl -benzene	-	-	-	-	0.3 (2.3)	0.4 (2.6)	0.1 (1.8)	-	-	-
32	2-Methyl- benzofuran	0.5 (4.5)	-	-	-	-	-	-	-	-	-
	Total	11.1	13.6	18.3	12.8	13.0	15.4	5.7	28.3	26.8	25.4

[a]: plausible portion of each compound in oil

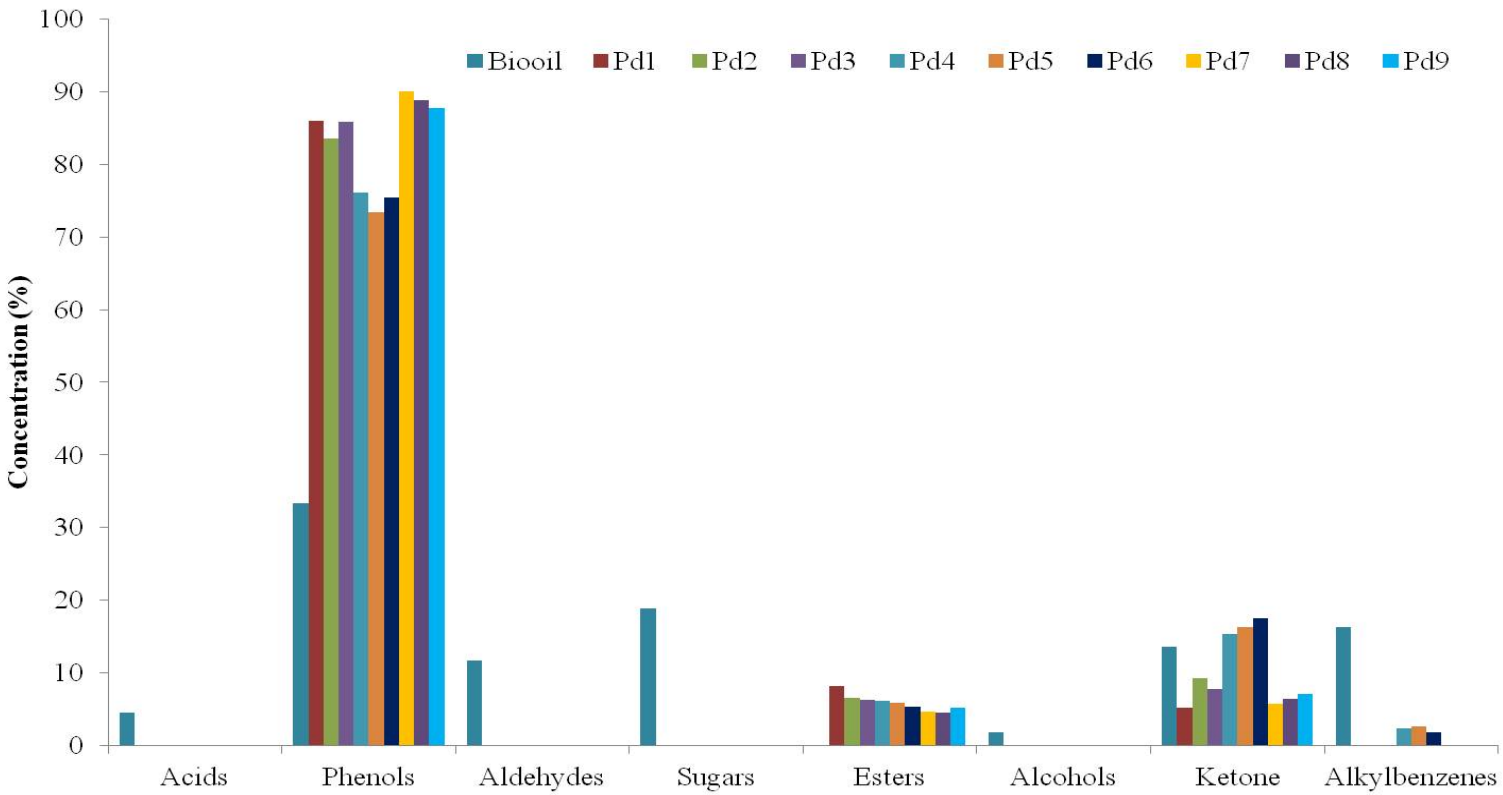

Figure 5. Distribution of compounds in heavy oil performed with Pd/C at 45 min (Reaction temperature: 250, 300 and 350°C, Catalyst: 4 wt%, Ethanol/bio-oil ratio: 1/4 (w/w), H_2 pressure: 30 bar)

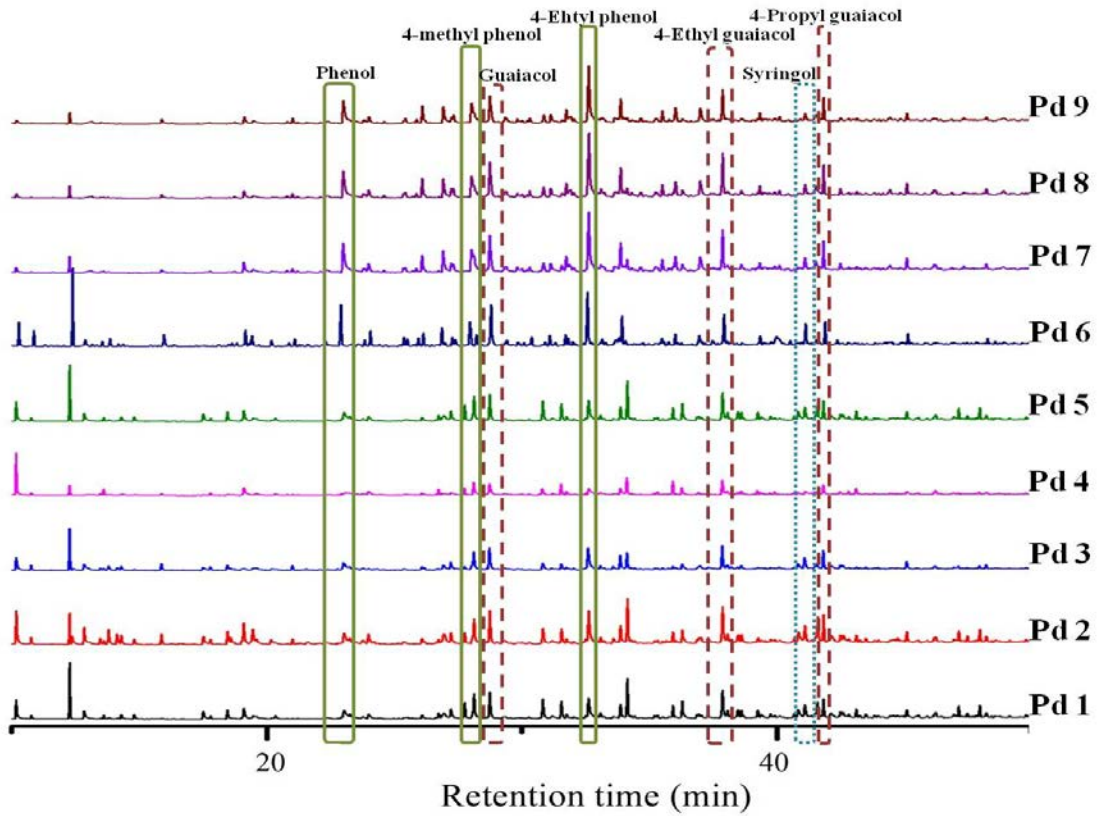

Figure 6. Gas chromatogram of Pd1-9

Table 5. Plausible chemical modification routes during HDO of bio-oil

Plausible chemical modification	Hydrodeoxygenation	
	Reactant in bio-oil	Product in heavy oil
Demethoxylation	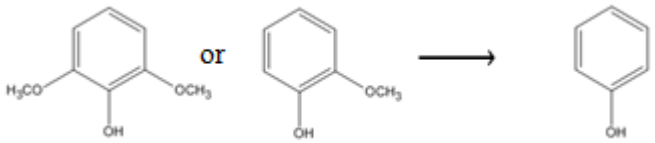 14. Syringol 5. Guiacol	2. Phenol
Hydrogenation	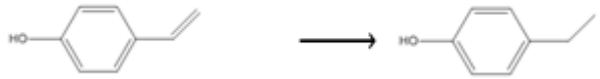 10. 4-Vinyl-phenol	7. 4-Ethyl-phenol
Dealkylation	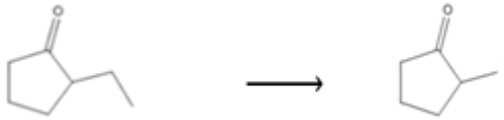 29. 2-Ethyl-cyclopentanone	26. 2-Methyl-cyclopentanone
Dealkylation via ring opening	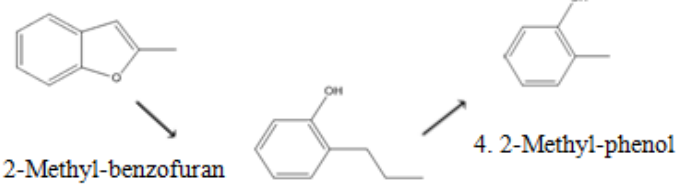 37. 2-Methyl-benzofuran 11. 2-Propyl-phenol	4. 2-Methyl-phenol
Dealkylation via hydrogenation	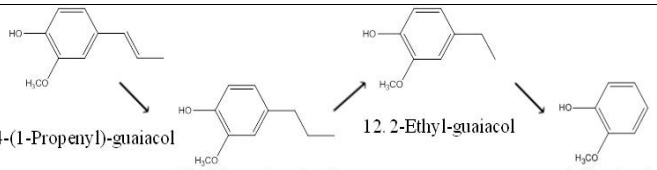 17. 4-(1-Propenyl)-guaiacol 15. 4-Propyl-guaiacol 12. 2-Ethyl-guaiacol	5. Guaiacol
Hydrogenation, decarbonylation, dehydroxylation and ring opening	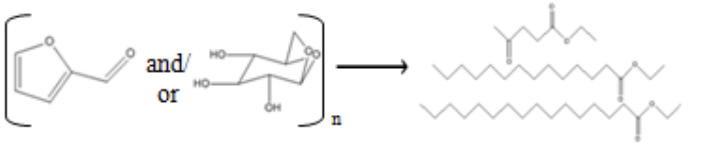 18. Furfural 19. Levoglucosan	20. 4-oxo-pentadecanoic acid, ethyl 21. Hexadecanoic acid, ethyl ester 22. Octadecanoic acid, ethyl ester

4.1.3. Macromolecules transition from bio-oil to heavy oil

4.1.3.1. Physicochemical properties

Macromolecules extracted from bio-oil are called pyrolytic lignin (PL). Those in heavy oil are referred to as phenol polymers (PP) in this study. When bio-oil is produced from woody biomass, those macromolecular lignin fragments amount to ca. 22.4 wt% and are assumed to be the main reason for the increase in the viscosity and instability of bio-oil. Therefore, many lignin fragments result from a decline in efficiency during combustion in engines (Bayerbach & Meier, 2009). A previous study showed that a HDO reaction with supercritical ethanol effectively converted macromolecules, which resulted in improved heavy oil properties (Tang et al., 2010). As confirmed previously, Pd4-6 were selected to extract phenol polymers (called Pd PP1-3, respectively) since they had high yield, high HHV and few unstable compounds. PL was also extracted and compared with Pd PP1-3. Typical chemical properties of those are presented in Table 5.

Yields of PP based on the weight of bio-oil were 9.3 and 8.8% for 1 and 2, which comprise 41.5 and 39.3% of PL, respectively. The reaction time was extended to 60 min (Pd6), the yield increased to 17.7% (Pd PP3). The decrease in PP was indirect evidence that bio-oil became stable through the HDO reaction. The carbon content of extracted PP increased to 73.3-75.4% compared with that of PL (65.0 wt%). The oxygen content of Pd PP1-3 decreased to 17.2-19.2 wt%, compared with that of PL (27.8 wt%). Both phenolic hydroxyl and methoxyl groups, generally known as major functional groups of those lignin derived phenols (Prochazkova et al., 2007), were drastically decreased from 6.8 and 11.6% in PL to 4.0-5.0 and 1.7-0.7% in Pd

PP1-3, respectively. While phenolic hydroxyl groups showed no significant differences with reaction time, methoxyl groups were visibly decreased with increasing reaction time. This suggested that demethoxylation was one of the major reactions of deoxygenation and easily occurred at the above experimental conditions, while dehydroxylation of phenolic hydroxyl groups required more kinetic energy than was available under those conditions (Gutierrez et al., 2009).

Table 6. Characteristics of lignin fragment extracted from Pd4-6

Lignin fragment	Yield (%)	Elemental analysis (wt%)				Average molecular Weight			Functional groups (%)	
		C	H	N	O	M_w (Da)	M_n (Da)	PDI(M_w/M_n)	Phen-OH	OCH_3
PL	22.4	65.0	6.4	0.6	27.8	1,065	544	2.0	6.8(0.6)[b]	11.6(1.1)
Pd PP1	9.3(19.0)[a]	74.5	6.9	0.6	17.7	1,316	481	2.7	4.0(0.5)	1.7(0.5)
Pd PP2	8.8(21.1)	73.3	6.8	0.6	19.2	1,165	304	3.8	5.1(0.2)	1.0(0.1)
Pd PP3	17.1(45.7)	75.4	7.1	0.6	17.2	1,093	353	3.1	5.0(0.0)	0.7(0.0)

[a]: Based on the weight of bio-oil.
[b]: standard deviation

4.1.3.2. Structural transition of lignin fragment during HDO

PL and Pd PP1-3 were subjected to nitrobenzene oxidation (NBO) to measure the ether linkages (non-condensed) in macromolecules. After NBO was completed, different types of C6C1 phenols, mainly vanillin and vanillic acid from G-type lignin, syringaldehyde and syringic acid from S-type lignin and a small amount of 4-hydroxy-benzaldehyde and 4-hydroxy-benzoic acid from H-type lignin, were produced from lignin fragments. The amount of those essential products is shown in Table 6. The total concentration of H-, G- and S-type phenol compounds decreased from 1679.5 μmol/g in PL to 30.6-61.9 μmol/g in Pd PP1-3 (Table 6). Approximately 96.3-98.2% of the ether linkage in PL cleaved or was modified during HDO. As reaction time increased, G-type compounds decreased (34.1-21.1 μmol/g) and H-type compounds increased (0.0-11.1 μmol/g). Considering decreasing G- and S-type derivatives (23.4-21.9 and 9.0-7.0%, respectively) and increasing H-type derivatives (53.3-55.7%) with increasing reaction time (Table 7), it was verified that demethoxylation sequentially occurred. Coinciding with Mw (increased from 1065 Da in PL to 1093-1316 Da in Pd PP1-3), PL was simultaneously condensed with cleavage of ether linkages (Kim et al., 2012). Also the lower S/G ratio of phenol polymers (0.0-1.1) compared with that of PL (2.6) suggests that ether linkages connecting S-types were easily cleaved compared with those between G-types (Wikberg & Liisa Maunu, 2004).

Thermal degradation properties of macromolecules were investigated using an analytical pyrolyzer-GC/MS. The analytical pyrolyzer-GC/MS has been proven to be a powerful instrument for investigation of thermal degradation properties of biomass. Moreover, it can identify pyrolytic compounds before condensation reactions start (Fahmi et al., 2007). Thus, it was used to identify

thermal degradation products as well as the level of macromolecules in this study. Approximately 30 kinds of thermal degradation products released from macromolecules were identified by comparison with a mass spectra library, and those compounds are listed in Table 7. Thermal degradation products indirectly showed that the comprehensive difference between the structures of two macromolecules may change during the HDO process. PL mainly produced unsaturated phenols such as p-vinyl-phenol and p-vinyl-guaiacol, whereas PP released saturated phenols such as p-cresol, 4-ethyl-phenol and 4-propyl-guaiacol. The latter compounds can be assumed to be formed from hydrogenation of those in PL during the HDO process. In addition, their relative yield decreased by approximately 19.9-33.5% after the HDO process. This might be associated with condensation of macromolecules during the HDO process. Also the GC-FID chromatogram in Fig. 4 described decreasing amounts of unsaturated compounds such as p-vinyl-phenol, p-vinyl-guaiacol and 4-(2-propenyl)-syringol as well as phenol. According to this hypothesis, condensation of each macromolecule might occur at the site of the unsaturated carbon and demethoxylated carbon (Argyropoulos & Sun, 1996) with hydrogenation during the reaction.

FT-IR spectra of macromolecules are shown in Fig. 5, but no significant differences could be found. Fig. 5 shows typical lignin bands such as those at 3378, 2924, 1702, 1513, 1113 and 1033 cm^{-1}, which imply O-H stretching, C-H in methyl, C=O in ester groups, aromatic skeleton vibration and aromatic C-H in the S-unit and G-unit, respectively (Lin & Dence, 1992). One minor change is that peaks showing aromaticity (1513, 1113 and 1033 cm^{-1}) were decreased, while methyl and ester groups increased (2924 and 1702 cm^{-1}). This was illustrative of deformation of macromolecules during HDO.

Table 7. Determination of essential nitrobenzene oxidation products of phenol polymer

Lignin fragment	Amount(μmol/g)							
	4-Hydroxy benzaldehyde	4-Hydroxy benzoic acid	Vanillin	Vanillic acid	Syringaldehyde	Syringic acid	Total	S/G ratio
PL	15.4(0.3) [a]	0.0(0.0)	279.5(5.1)	181.3(9.5)	937.1(32.8)	263.8(0.6)	1679.5(50.5)	2.6
Pd PP1	0.0(0.0)	0.0(0.0)	0.0(0.0)	30.6(2.3)	0.0(0.0)	0.0(0.0)	30.6(2.3)	0.0
Pd PP2	0.0(0.0)	0.0(0.0)	0.0(0.0)	34.1(0.0)	0.0(0.0)	27.8(5.6)	61.9(5.6)	0.8
Pd PP3	11.1(3.3)	0.0(0.0)	0.0(0.0)	21.1(3.3)	0.0(0.0)	25.7(1.7)	57.9(8.3)	1.1

[a]: standard deviation

Table 8. Quantitative analysis of low molecular weight components in lignin fragment (Pd PP1-3)

No.	RT	Compounds	Source[a]	PL	Pd PP1	Pd PP2	Pd PP3
1	16.7	2-Methyl-2-cyclopentenone	C	0.0	0.5	0.4	0.5
2	20.0	Phenol	H	1.9	0.9	0.9	0.9
3	22.4	2-Hydroxy-3-methyl-2-cyclopenteneone	C	0.4	0.0	0.0	0.0
4	23.2	2,3-Dimethyl-2-cyclopentenone	C	0.0	0.6	0.5	0.7
5	23.8	o-Cresol	H	0.4	0.5	0.5	0.5
6	24.8	p-Cresol	H	2.1	1.6	1.5	1.5
7	25.7	Guaiacol	G	1.1	0.8	0.9	1.1
8	28.6	2,4-Dimethylphenol	H	0.3	0.5	0.4	0.5
9	29.5	4-Ethylphenol	H	2.0	1.3	1.7	3.0
10	30.1	2,3-Dimethylphenol	H	0.0	0.2	0.3	0.3
11	30.7	1,2-Benzenediol	H	0.6	0.5	0.4	0.3
12	31.0	p-Creosol	G	1.9	1.2	1.3	1.2
13	32.2	p-Vinylphenol	H	4.0	0.4	0.4	0.4
14	32.7	p-Isopropylphenol	H	0.2	0.3	0.3	0.4
15	33.3	4-Ethyl-m-Cresol	H	0.2	0.4	0.4	0.5
16	34.6	3-Methoxy-1,2-benzenediol	G	0.4	0.2	0.2	0.2
17	35.7	4-Ethyl-guaiacol	H	1.3	1.3	1.4	1.7
18	36.0	4-Methyl-1,2-benzenediol	H	0.5	0.4	0.4	0.4
19	37.9	p-Vinyl-guaiacol	G	2.4	0.3	0.3	0.2
20	38.6	2-Methyl-6-propylphenol	H	0.0	0.3	0.3	0.3
21	40.0	Syringol	S	0.6	0.4	0.5	0.5
22	40.5	p-Isobutyl-phenol	H	0.6	0.3	0.5	0.5
23	41.0	4-Propyl-guaiacol	G	0.2	1.3	1.3	1.6
24	46.0	4-Methyl-syringol	S	0.6	0.3	0.2	0.3
25	46.5	4-(1-Propenyl)-guaiacol	G	1.2	0.1	0.0	0.1
26	56.9	4-Propyl-syringol	S	0.0	0.7	0.4	0.4
27	63.1	4-(2-propenyl)-syringol	S	0.7	0.1	0.0	0.2
28	72.3	Hexadecanoic acid	C	0.9	0.3	0.5	0.8
29	73.1	Ethyl hexadecanoate	C	0.1	0.7	0.8	0.3
Sum of G-type lignin derivatives				7.2	3.9	4.0	4.4
Sum of S-type lignin derivatives				1.9	1.5	1.1	1.4
Total				**24.6**	**16.4**	**16.7**	**19.3**

[a]: C, carbohydrate derivatives; H, lignin p-hydroxyphenyl type derivatives; G, lignin guaiacyl type unit derivatives; S, lignin syringyl type derivatives

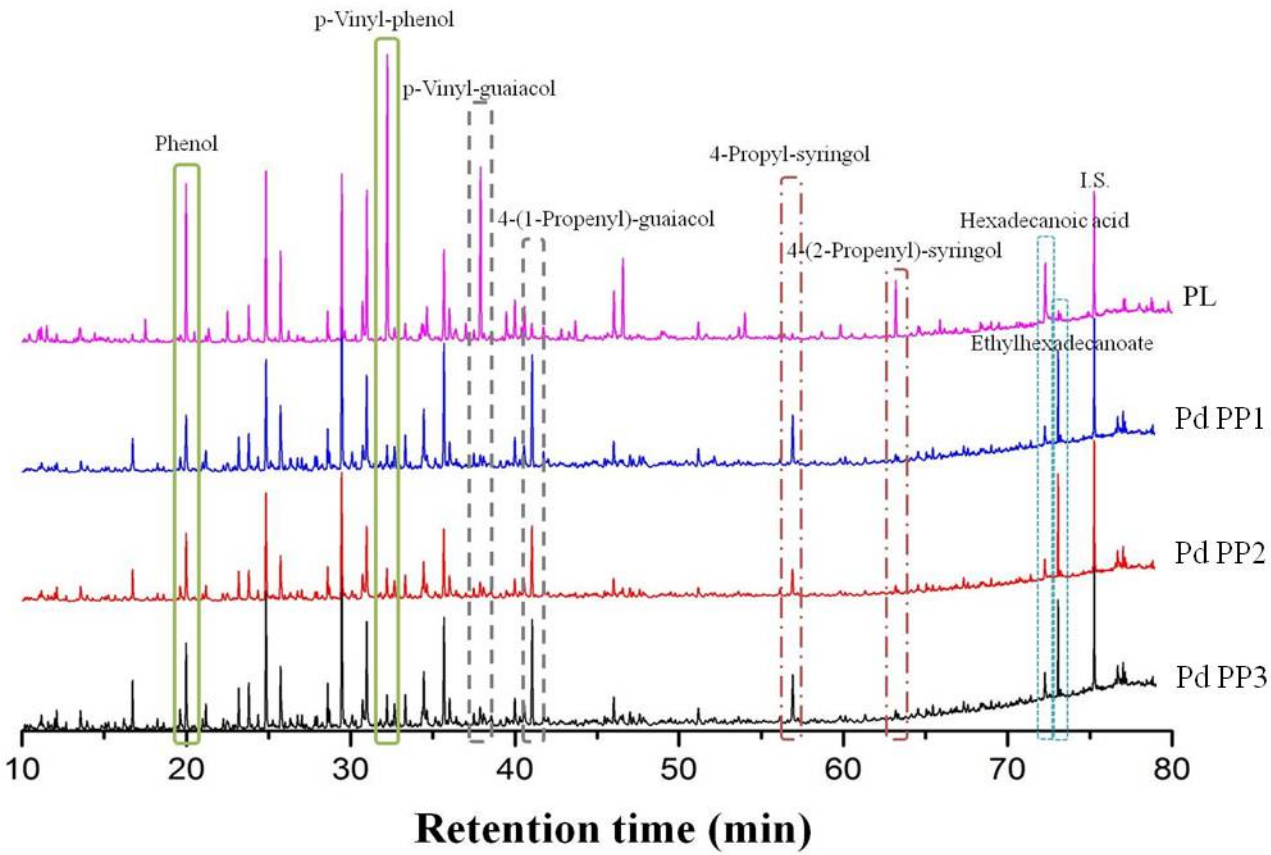

Figure 7. Gas chromatograms of lignin fragments (Pd PP1-3)

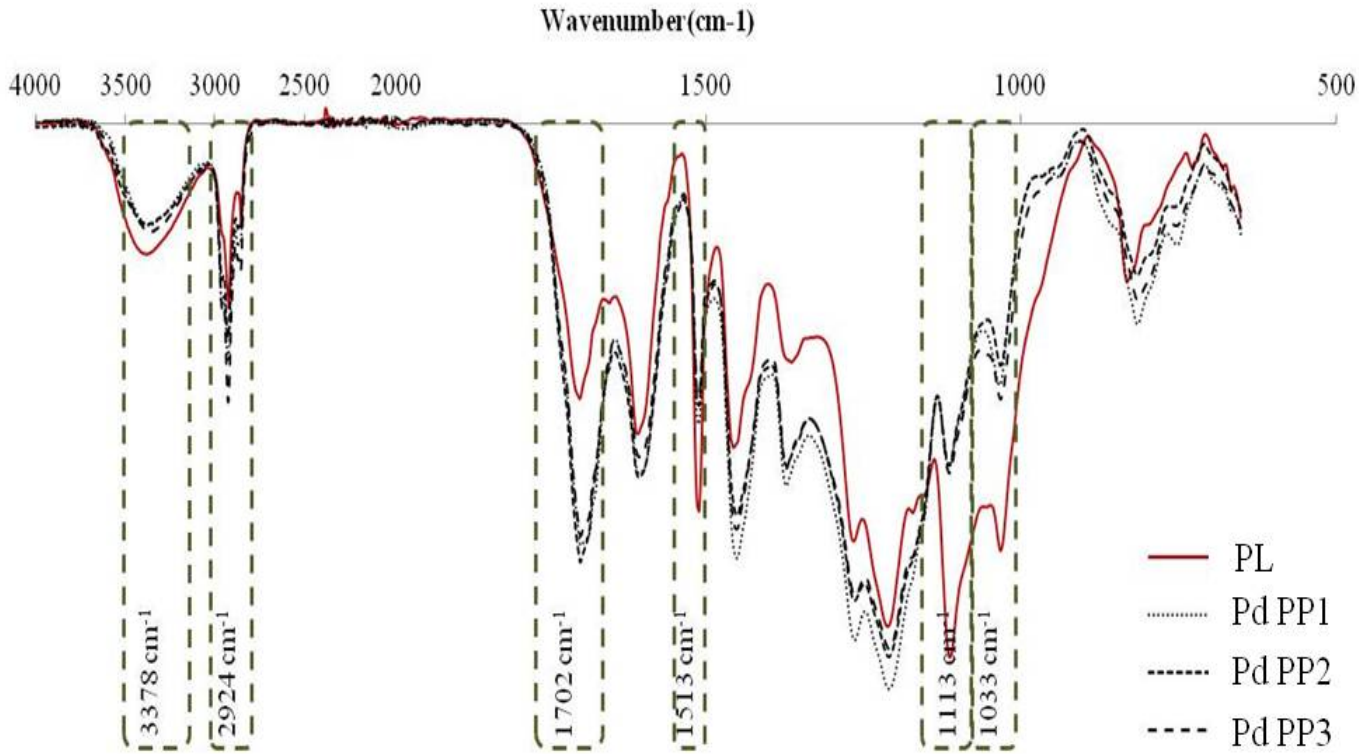

Figure 8. FT-IR spectra of Pd PP obtained from heavy oil

4.2. Bio-oil modifications during HDO with Ru/C catalyst

4.2.1. Mass balance of hydrodeoxygenation products

4.2.1.1. Influence of reaction temperature

The HDO reaction was performed at 250, 300 and 350°C with Ru/C to investigate the effect of reaction temperature on the HDO of bio-oil with Ru/C. The yield of each product was based on the weight of bio-oil as function of temperature, as shown in Table 9.

The yield of each product revealed that the composition of HDO products was considerably affected by temperature. A target product, heavy oil (Ru1-9), was definitely affected by reaction temperature. As shown in Table 9, the yield of heavy oil ranged between 27.9-54.3% based on the weight of bio-oil. The yield of heavy oil also gradually decreased with increasing reaction temperature, from 54.3 to 27.9% (30 min), from 49.2 to 28.4% (45 min) and from 40.6 to 30.4% (60 min). On the other hand, light oil yield increased or remained similar with increasing reaction temperature from 28.1 to 36.6% at 30 min, from 32.8 to 41.6% at 45 min, from 40.7 to 36.7% at 60 min, compared with heavy oil. Since light oil had high water content, this trend might be a result of dehydration of organic compounds in the oil phase to solvent based light oil (de Miguel Mercader et al., 2011). The yield of gas increased up to 350°C, especially at a reaction time of 30 min (from 7.6 to 23.0%). This trend resulted from further decomposition of organic compounds in the liquid phase (consisting mainly of organics in heavy oil) (Joshi & Lawal, 2012). At 45 min, the yield of char contemporaneously increased from 8.4 to 14.0% with increasing reaction temperature. As similar trend was noted

at 30 and 60 min. These results indicate that Ru/C accelerated both polymerization and further decomposition, leading to an increase in gas and char yields with increasing reaction temperature.

4.2.1.2. Influence of reaction time

As in case of results obtained using Pd/C, reaction time for experiments usign Ru/C was controlled (30, 45 and 60 min) at 250, 300 and 350°C, respectively. As shown in Table 9, the yield of heavy oils steadily decreased from 54.3 to 40.6% at 250°C, while it increased with increasing reaction time from 37.1 to 40.3% and from 27.9 to 30.4% at 300 and 350°C, respectively. Changes in heavy oil yield were accompanied by an increase in gas yield, at 250°C, gas yield increased from 7.6% at 30 min to 11.3% at 60 min while char yield showed no significant relationship with reaction time. Based on these results, it can be seen that Ru/C accelerated further decomposition with increasing reaction time; this is different from the case of Pd/C, which accelerated both polymerization and further decomposition. Bio-oil hydrogenated with Ru/C was therefore affected by both reaction temperature and time, though the related level was dissimilar between the two catalysts.

Table 9. The distribution of product yields as a function of reaction temperature and reaction time (wet basis, Ru/C catalyst loading: 4wt%, H_2 pressure: 30 bar)

Yield (%)	Ru1	Ru2	Ru3	Ru4	Ru5	Ru6	Ru7	Ru8	Ru9
	250°C 30min	250°C 45min	250°C 60min	300°C 30min	300°C 45min	300°C 60min	350°C 30min	350°C 45min	350°C 60min
Char	9.1 (0.0)[a]	8.4 (0.1)	9.6 (0.2)	9.1 (0.0)	10.4 (0.2)	7.9 (2.4)	13.0 (2.6)	14.0 (0.1)	9.0 (0.4)
Light oil	28.1 (0.3)	32.8 (0.4)	40.7 (2.3)	36.7 (0.1)	35.3 (1.2)	35.1 (2.0)	36.6 (3.4)	41.6 (0.9)	36.7 (3.1)
Heavy oil	54.3 (2.7)	49.2 (0.3)	40.6 (0.7)	37.1 (1.5)	38.2 (0.2)	40.3 (0.5)	27.9 (0.0)	28.4 (1.2)	30.4 (0.0)
Gas	7.6 (1.0)	9.6 (0.6)	11.3 (0.3)	17.0 (1.4)	16.2 (1.1)	16.7 (0.9)	23.0 (0.0)	16.1 (1.9)	24.0 (2.7)

[a]: Standard deviation

4.2.2. Characterization of heavy oil

4.2.2.1. Physicochemical properties

After HDO performed with Ru/C, the properties of bio-oil might be altered as it did with Pd1-9. Table 10 outlines physicochemical properties of bio-oil obtained after HDO. Water content decreased from 17.7% in bio-oil to 0.4-8.2% in Ru1-9 after the HDO reaction. When Ru/C was used for HDO, this was clearly affected by reaction time. Water content decreased slightly with increasing reaction time, from 8.2 (30 min) to 0.5% (60 min) at 250°C. As similar tendency was evident at 300 and 350°C. This tendency was elucidated as the dehydration of the organic phase improved with increasing reaction temperature (Mohan et al., 2006). However, the relationship between temperature and water content was only investigated at 45 min (8.2-2.1% at 30 min; 6.8-2.3% at 45 min). Since the activation of Ru/C is favored at lower temperature (Gutierrez et al., 2009), compared with Pd/C, mild temperatures and long reaction times are suitable for HDO with Ru/C.

The pH value of bio-oil (2.5) increased to 4.4-5.4 in heavy oil, with no significant differences between conditions. As in case of Pd1-9, it could be expected that acids derived from the decomposition of carbohydrates might be altered into desired compounds like esters and ketones. Viscosity decreased from 29.6 cSt for bio-oil to 3.0-5.7 cSt for Ru1-9, similar to values reported in previous studies and to those for Pd1-9.

Carbon content in bio-oil (40 wt%) increased to 54.8-71.4 wt% in heavy oils while oxygen content decreased from 52.2 wt% in bio-oil to 20.9-35.8 wt% in Ru1-9. Ru6 and 9 (60 min at 300 and 350°C), in particular showed relatively high carbon levels of 66.0-71.4 wt%, and low oxygen levels of 20.9-25.1 wt%, compared with those of other Ru oils and Pd1-9. These results were caused by conversion of oxygenated compounds in bio-oil to gas or light oil phases at high temperatures, as well as by dehydration (Nimmanwudipong

et al., 2011). The above results also resulted in higher HHVs of Ru6 and 9 (26.1-26.7 MJ/kg) compared with those of bio-oil (17.3 MJ/kg), other Ru oils (23.3-24.9 MJ/kg) and Pd1-9 (22.8-24.2 MJ/kg). This indicates that deoxygenation became predominant with increasing reaction temperature and long reaction times.

As described in Fig. 9, the O/C ratio of bio-oil (1.0) decreased to 0.2-0.5 due to deoxygenation after HDO. The H/C ratio of bio-oil (2.2) also decreased to 1.2-2.1. Ru1-9 all showed a well-deoxygenated state compared with bio-oil, and similar results were achieved with Pd1-9. The O/C ratio of Ru8 was 0.2, which was the most deoxygenated, coincided with a decrease in H/C ratio (1.2). When the H/C ratio increased to 1.7-1.9, the O/C ratio decreased to 0.4. In concludsion, hydrogenation and deoxygenation might occur on similar active sites on noble metal and activated carbon (Zhao et al., 2009). It is therefore still necessary to find a catalyst, sustaining the H/C ratio with reducing O/C ratio.

Table 10. Physicochemical properties of bio-oil and heavy oils (wet basis, Ru/C catalyst loading: 4wt%, H_2 pressure: 30bar)

	Bio-oil	Ru1	Ru2	Ru3	Ru4	Ru5	Ru6	Ru7	Ru8	Ru9
Water content (wt%)	17.7	8.2	6.8	0.5	2.5	2.1	1.4	2.1	2.3	1.7
pH	2.5	4.4	4.4	5.0	5.0	5.2	5.4	4.8	5.3	5.2
Viscosity(cSt)[a]	29.6	4.5	5.7	5.7	3.8	4.4	3.5	4.1	3.0	5.1
C (wt%)	40.0	59.5	58.3	54.8	60.8	57.9	66.0	59.4	56.1	71.4
H (wt%)	7.5	8.5	8.3	9.1	9.0	9.4	8.5	8.9	9.7	7.1
N (wt%)	0.2	0.3	0.2	0.2	0.3	0.3	0.4	0.3	0.2	0.5
O[b] (wt%)	52.2	31.7	33.1	35.8	29.8	32.3	25.1	31.3	34.0	20.9
S (wt%)	0.2	0.0	0.0	0.1	0.1	0.1	0.1	0.1	0.1	0.1
HHV(MJ/kg)[c]	17.3	24.3	23.8	23.3	24.9	24.4	26.1	24.5	24.1	26.7

[a]:Measured at 40°C
[b]:Calculated by difference
[c]:High heating value was calculated following formula,
HHV(MJ/kg) = -1.3675 + (0.3137 X C) + (0.7009 X H) + (0.0318 X O)

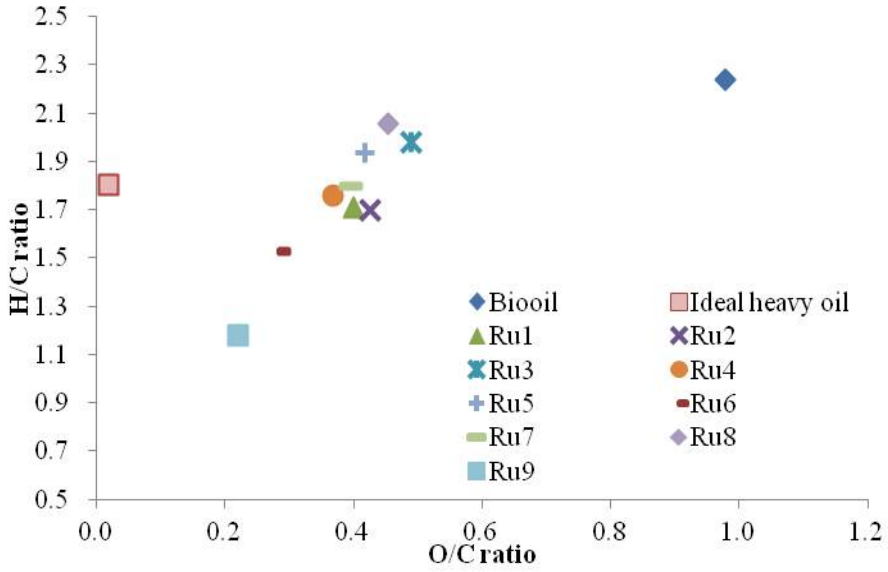

Fig 9. Van Krevelen diagram of bio-oil, heavy oils performed with Ru/C

4.2.2.2. Qualification and modification of low molecular compounds

A total of 32 kinds of micromolecules in oils were identified from GC/MS analysis. Ru1-9 mainly consisted of various monomeric phenols such as phenol, guaiacol and 4-ethyl-phenol. Micromolecules were classified according to their functional groups. The distribution of the relative concentration of classified micromolecules is shown in Fig. 10. Common changes found to occur during the reaction included decrease in acids, aldehydes, sugars and alkylbenzenes and increase in esters and ketones, with these changes very similar to those occuring in Pd1-9. However, low molecule concentrations were recorded in Ru4-6, as compared with other Ru oils, with this finding also opposed to that for Pd1-9.

Table 11 provides a detailed list of micromolecules in Ru1-9. Ru3 showed a 35.1% decrease and Ru9 a 56.8% increase in micromolecules compared with bio-oil, respectively. Strikingly, phenols increased by 2.2-2.6 times increased, compared with bio-oil. Typically unsaturated 4-vinyl-phenol (2.7%) and 4-(1-propenyl)-guaiacol (1.8%) in bio-oil decreased while 4-ethyl-phenol (9.2-18.7%), 4-methyl-guaiacol (7.1-15.7%) and 4-propyl-guaiacol (3.5-7.3%) increased in Ru1-9. Moreover, phenol and 4-methyl phenol, not detected in bio-oil, comprised 1.4-11.4% and 3.7-55% of the final product after HDO, respectively, via demethoxylation, demethylation and hydrogenation. Evidently, unstable and undesired 2-hydroxy-butanoic acid, furfural, levoglucosan and butandial in bio-oil were removed or converted to relatively stable esters in Ru1-9, such as 4-oxo-pentanoic acid ethyl ester, hexadecanoic acid ethyl ester and octadecanoic acid ethyl ester. This might be due to hydrogenation, decarbonylation, dehydroxylation and ring opening, also noted in the case of Pd1-9.

Based on GC/MS analysis, plausible chemical modifications such as demethoxylation, hydrogenation, dealkylation, ring opening, decarbonylation and dehydroxylation were assumed to have occurred. The 1.4-11.4% of

phenol identified only after HDO could be derived from demethoxylation of guaiacol and syringol (Bui et al., 2011). Regardless of demethoxylation of guaiacol and syringol to phenol, guaiacol (7.3%) and syringol (1.6%) in bio-oil increased by 2.9-16.6% and 5.2-9.3% in Ru1-9, respectively. This was due to dealkylation via hydrogenation (Furimsky et al., 1986) and was confirmed by elimination of 4-methyl-syringol (0.8%) and 4-(1-propenyl)-guaiacol (1.6%) in bio-oil. The range of amounts of guaiacol and syringol was larger than that of Pd1-9. In addition, phenol, 4-ethyl phenol, 4-methyl guaiacol and 4-ethyl guaiacol also exhibited a wide concentration range compared with results for Pd/C. Based on the above, it would appear that the degree of demethoxylation and dealkylation of Ru/C in bio-oil is relatively sensitive to reaction conditions, in contrast to Pd/C. 2-methyl-phenol (3.2-3.8%) in Ru1-9 was formed by dealkylation via ring opening (Furimsky, 2000; Liu et al., 2012b) of 2-methyl-benzofuran (4.1%) in bio-oil. Its concentration was higher than that of Pd1-9. Considering that 2-propyl-phenol, an intermediate of the above reaction, remained more evenly concentrated in Ru1-9 (1.1-4.6%) compared with Pd1-9 (1.7-10.8%), dealkylation of Ru/C occurred to a better degree than in the case of Pd/C under these HDO conditions.

Table 11. Quantitative analysis of low molecular weight components in bio-oil and heavy oil (wet basis, Ru/C catalyst loading: 4wt%, H_2 pressure: 30bar)

	Compound	Relative area(peak area/ I.S. area)									
		Bio-oil	Ru1	Ru2	Ru3	Ru4	Ru5	Ru6	Ru7	Ru8	Ru9
	Acids										
1	Butanoic acid, 2-hydroxy-	0.5 (4.5)[a]	-	-	-	-	-	-	-	-	-
	Phenols										
2	Phenol	-	1.0 (7.9)	1.1 (9.1)	0.1 (1.4)	0.8 (9.4)	0.9 (9.1)	0.9 (11.4)	1.2 (8.8)	0.7 (10.9)	2.0 (11.4)
3	2-Methyl-phenol	-	0.5 (3.8)	0.5 (3.7)	0.4 (5.0)	0.3 (3.8)	0.4 (3.9)	0.3 (3.7)	0.6 (4.6)	0.3 (4.4)	1.0 (5.5)
4	4-Methyl-phenol	-	0.6 (4.5)	0.7 (5.4)	0.5 (6.3)	0.5 (5.5)	0.5 (5.4)	0.6 (7.2)	0.7 (5.2)	0.5 (8.4)	1.7 (9.7)
5	Guaiacol	0.9 (8.1)	1.5 (12.1)	1.6 (12.4)	1.2 (16.6)	1.3 (14.8)	1.4 (15.0)	0.4 (4.6)	0.4 (2.9)	0.8 (13.5)	1.6 (9.4)
6	2,4-Dimethyl-phenol	-	0.1 (1.1)	0.2 (1.7)	0.2 (2.3)	0.1 (1.1)	0.2 (1.8)	0.1 (1.6)	0.3 (2.0)	0.2 (2.6)	0.6 (3.5)
7	4-Ethyl-phenol	0.3 (2.7)	1.2 (9.2)	1.3 (10.7)	1.0 (13.9)	1.2 (13.6)	1.2 (13.0)	1.2 (15.5)	2.6 (18.7)	0.9 (15.1)	3.2 (18.2)
8	2,3-Dimethyl-phenol	0.3 (2.7)	-	-	-	-	-	-	-	-	-
9	4-Methyl-guaiacol	0.3 (2.7)	1.8 (14.4)	2.0 (15.7)	0.7 (9.3)	0.6 (7.3)	0.7 (7.8)	0.7 (8.7)	2.1 (15.1)	0.4 (7.1)	1.3 (7.5)
10	4-Vinyl-phenol	0.3 (2.7)	-	-	-	-	-	-	-	-	-
11	2-Propyl-phenol	0.3 (2.7)	0.1 (1.1)	0.2 (1.7)	-	0.1 (1.1)	0.2 (2.4)	0.2 (2.2)	0.6 (4.6)	0.1 (2.3)	0.8 (4.6)
12	4-Ethyl-guaiacol	0.2 (1.8)	1.0 (7.8)	0.9 (7.5)	0.7 (9.3)	0.8 (9.5)	0.8 (8.7)	0.7 (9.4)	1.3 (9.3)	0.5 (7.8)	1.3 (7.2)
13	Syringol	0.2 (1.8)	1.0 (7.8)	1.1 (8.5)	0.7 (9.3)	0.7 (7.7)	0.7 (7.6)	0.6 (7.6)	0.8 (5.5)	0.3 (5.2)	0.7 (4.0)
14	4-Propyl-guaiacol	0.6 (5.4)	0.4 (3.5)	0.5 (3.7)	0.4 (5.2)	0.6 (7.3)	0.6 (6.2)	0.5 (6.6)	0.8 (6.1)	0.3 (5.2)	0.7 (4.2)
15	4-Methyl-syringol	0.1 (0.9)	-	-	-	-	-	-	-	-	-
16	4-(1-Propenyl)-guaiacol	0.2 (1.8)	-	-	-	-	-	-	-	-	-
	Aldehydes										
17	Furfural	1.3 (11.7)	-	-	-	-	-	-	-	-	-
	Sugars										
18	Levoglucosan	2.1 (18.9)	-	-	-	-	-	-	-	-	-
	Esters										
19	Pentanoic acid, 4-oxo-, ethyl ester	-	0.4 (3.5)	0.3 (2.8)	0.3 (3.9)	0.2 (2.0)	0.2 (2.1)	0.2 (2.9)	0.3 (2.1)	0.1 (1.2)	0.2 (1.1)
20	Hexadecanoic acid, ethyl ester	-	0.2 (1.4)	-	0.2 (3.0)	0.1 (1.1)	0.1 (1.6)	0.2 (2.0)	0.2 (1.4)	0.1 (1.7)	0.3 (1.6)
21	Octadecanoic acid, ethyl ester	-	-	-	-	-	-	-	-	-	-
	Alcohols										
22	Butanedial	0.2 (1.8)	-	-	-	-	-	-	-	-	-
	Ketone										
23	2-Methyl-cyclopentanone	-	0.2 (1.4)	0.2 (1.7)	0.1 (1.4)	0.1 (1.1)	0.1 (1.2)	0.1 (1.3)	0.2 (1.2)	-	0.1 (0.5)
24	2-Ethyl-cyclopentanone	-	-	-	-	0.1 (1.1)	0.1 (1.4)	0.2 (2.1)	0.1) (1.0	0.1 (1.6)	0.4 (2.4)
25	2,5-Hexanedione	-	0.3 (2.2)	0.2 (1.7)	0.1 (1.4)	0.1 (1.1)	0.1 (1.3)	0.1 (1.8)	0.2 (1.5)	0.1 (1.2)	0.1 (0.6)
26	2-Ethyl-2-cyclopentenone	0.4 (3.6)	1.6 (12.5)	1.1 (9.1)	0.6 (7.7)	0.5 (5.5)	0.4 (4.3)	0.4 (4.8)	0.6 (4.2)	0.2 (4.0)	0.3 (1.6)
27	2,3-Dimethyl-2-cyclopentenone	0.4 (3.6)	0.7 (5.8)	0.6 (5.0)	0.1 (1.4)	0.6 (7.3)	0.7 (7.2)	0.5 (6.6)	0.7 (5.4)	0.4 (7.0)	1.2 (6.8)
28	4-Hydroxy-5,6-dihydro-(2H)-pyranone	0.3 (2.7)	-	-	-	-	-	-	-	-	-
29	2-Hydroxy-3-methyl-2-cyclopentenone	0.4 (3.6)	-	-	-	-	-	-	-	-	-
	Alkylbenzenes										
30	1,3-Dimethyl- benzene	1.3 (11.7)	-	-	-	-	-	-	-	-	-
31	1,2,3-trimethoxy-5-methyl -benzene	-	-	-	-	-	-	-	-	-	-
32	2-Methyl- benzofuran	0.5 (4.5)	-	-	-	-	-	-	-	-	-
	Total	11.1	12.5	12.6	7.2	8.9	9.4	7.9	13.8	6.0	17.4

[a]: plausible portion of each compound in oil

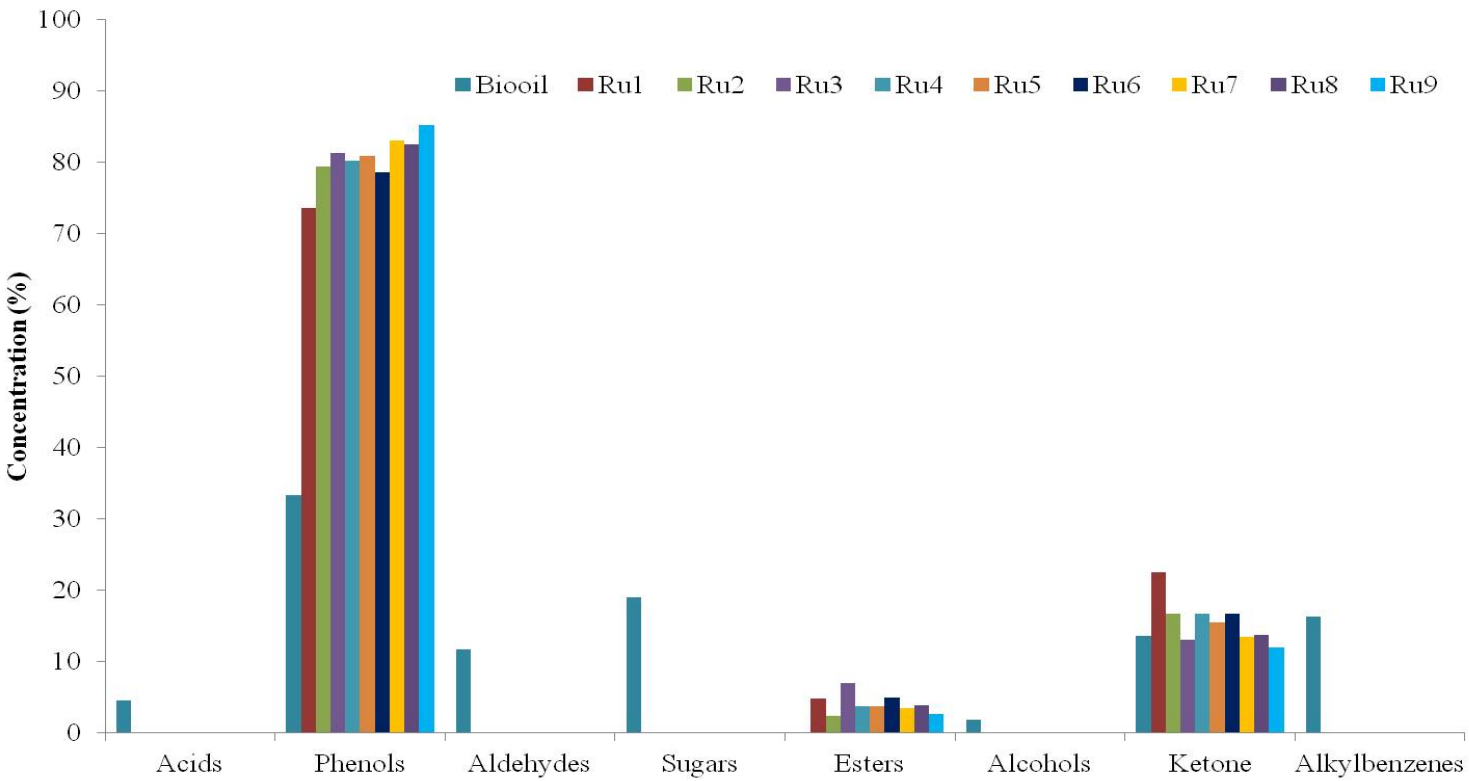

Figure 10. Distribution of compounds in heavy oil performed with Ru/C at 45 min (Reaction temperature: 250, 300 and 350°C, Catalyst: 4 wt%, Ethanol/bio-oil ratio: 1/4 (w/w), H_2 pressure: 30 bar)

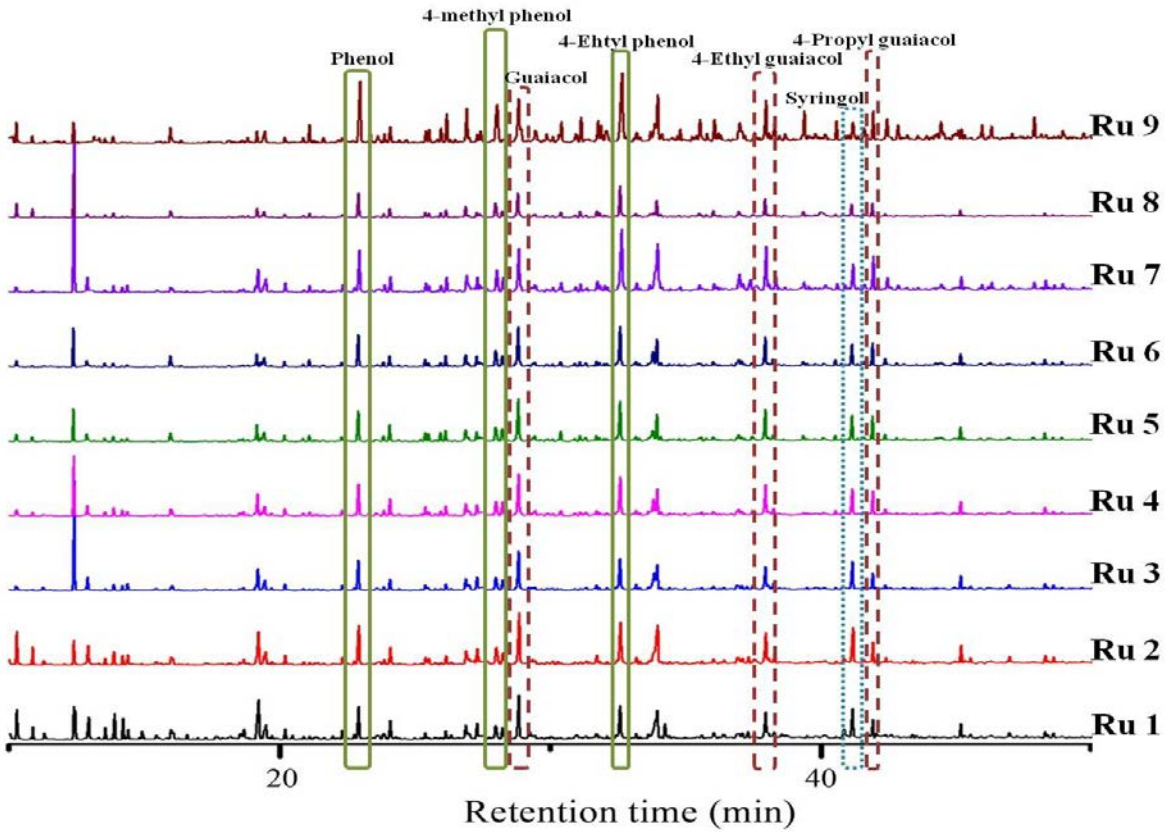

Figure 11. Gas chromatogram of Ru1-9

4.2.3. Macromolecules transition from bio-oil to heavy oil

4.2.3.1. Physicochemical properties

As confirmed in the Pd/C sections above (4.2.1.1 and 4.2.1.2), Ru4-6 were selected for the extract of phenol polymers (called Ru PP1-3, respectively); their typical chemical properties are shown in Table 12.

Yields of Ru PP1-3, based on the weight of bio-oil, were evenly at 7.8-9.0%. This constituted 34.8-40.2% of PL, which was less than that of Pd PPs from the same condition of heavy oils (8.8-17.7%). Notably, the yield of Ru PP3 (9.0%) was approximately half of Pd PP3 (17.7%). Since PL enhanced bio-oil instability, the reduction of PP yield after the HDO reaction was indirect evidence that oil stability had improved. The carbon content of Ru PP1-3 increased to 75.7-77.4% compared with PL (65.0 wt%), and was even higher than that of Pd PP (73.3-75.4%). The oxygen content of Ru PP1-3 decreased to 15.3-17.6 wt%, compared with that of PL (27.8 wt%). Both phenolic hydroxyl and methoxyl groups decreased from 6.8 and 11.6% in PL to 5.0-6.1 and 0.1-0.2% in Ru PP1-3, respectively. While phenolic hydroxyl groups showed no significant differences, methoxyl groups visibly decreased during the HDO reaction. Average molecular weight also increased from 1065 in PL to 1174-1212 in Ru PP1-3 with a decrease in PDI (from 2.0 to 1.6-1.7) involving polymerization and decomposition. Through these macromolecular properties, parts of lignin fragments in bio-oil condensed with the C3 or C5 site, where methoxyl groups were demethoxylated during HDO (Argyropoulos & Sun, 1996). However, the condensation reaction might occur after almost regular an amount of demethoxylation is performed, during 30-60 min of HDO.

Table 12. Characteristics of lignin fragment extracted from Ru4-6

Lignin fragment	Yield (%)	Elemental analysis (wt%)				Average molecular Weight			Functional groups (%)	
		C	H	N	O	M_w (Da)	M_n (Da)	PDI (M_w/M_n)	Phe-OH	OCH_3
PL	22.4	65.0	6.4	0.6	27.8	1,065	544	2.0	6.8 (0.6)[c]	11.6 (1.1)
Ru PP1[b]	7.8 (21.0)[a]	76.7	6.6	0.0	16.8	1,199	735	1.6	6.1 (0.4)	0.2 (0.0)
Ru PP2[b]	8.8 (24.9)	75.7	6.8	0.0	17.6	1,174	708	1.7	5.4 (0.0)	0.1 (0.0)
Ru PP3[b]	9.0 (23.7)	77.4	7.3	0.0	15.3	1,212	709	1.7	5.0 (0.7)	0.1 (0.0)

[a]: Based on the weight of crude oil.
[b]: phenol polymer obtained from Ru4, 5 and 6, respectively
[c]: standard deviation

4.2.3.2. Structural transition of lignin fragment during HDO

Using the analytical pyrolyzer-GC/MS, pyrolytic compounds present before the start of condensation reactions (Fahmi et al., 2007) could be identified. Total 29 kinds of thermal degradation products released from macromolecules were identified by comparison with a mass spectra library, with these compounds listed in Table 13. Comprehensive different structures of PL and Ru PP1-3 were expected, on the basis of the varied thermal degradation products resulting from the HDO process. PL mainly produced unsaturated phenols such as p-vinyl-phenol, p-vinyl-guaiacol, 4-(1-propenyl)-guaiacol and 4-(2-propenyl)-syringol, whereas Ru PP1-3 released saturated phenols such as phenol, 4-ethyl-phenol, 4-ethyl guaiacol, 4-propyl-guaiacol, 4-methyl syringol and 4-propyl syringol, discrepancies between Pd PP1-3. 4-(2-propenyl)-syringol, 4-propyl-syringol and 4-methyl-syringol were not detected in Ru PP3. This might be also the evidence of condensation occurring after demethoxylation as previously mentioned. Other than this exception, other variations and component compositions of Ru PP1-3 were similar to those of Pd PP1-3.

The GC-FID chromatogram in Fig. 12 describes decreasing amounts of unsaturated compounds, such as p-vinyl-phenol, p-vinyl-guaiacol and 4-(2-propenyl)-syringol as well as of hexadecanoic acid. On the other hand, peaks that appeared for saturated and stable forms of components such as 4-ethyl phenol, 4-ehtyl guaiacol, 4-propyl-syringol and ethylhexadecanoate were strikingly enlarged.

Table 13. Quantitative analysis of low molecular weight components in lignin fragment (Ru PP1-3)

No.	RT	Compounds	Source[a]	PL	Ru PP1	Ru PP2	Ru PP3
1	16.7	2-Methyl-2-cyclopentenone	C	0.0	0.6	0.9	0.0
2	20.0	Phenol	H	1.9	1.2	1.5	0.9
3	22.4	2-Hydroxy-3-methyl-2-cyclopenteneone	C	0.4	0.6	0.9	0.0
4	23.2	2,3-Dimethyl-2-cyclopentenone	C	0.0	0.0	0.0	0.0
5	23.8	o-Cresol	H	0.4	0.6	0.6	0.0
6	24.8	p-Cresol	H	2.1	0.0	0.0	0.0
7	25.7	o-Guaiacol	G	1.1	1.2	1.5	0.0
8	28.6	2,4-Dimethylphenol	H	0.3	0.0	0.0	0.0
9	29.5	4-Ethylphenol	H	2.0	2.4	3.0	1.5
10	30.1	2,3-Dimethylphenol	H	0.0	0.0	0.0	0.0
11	30.7	1,2-Benzenediol	H	0.6	0.0	0.0	0.0
12	31.0	p-Creosol	G	1.9	1.5	1.8	1.2
13	32.2	p-Vinylphenol	H	4.0	0.6	0.6	0.0
14	32.7	p-Isopropylphenol	H	0.2	0.0	0.9	0.0
15	33.3	4-Ethyl-m-Cresol	H	0.2	0.3	0.6	0.0
16	34.6	3-Methoxy-1,2-benzenediol	G	0.4	0.0	0.0	0.0
17	35.7	4-Ethyl-guaiacol	H	1.3	1.5	2.1	1.2
18	36.0	4-Methyl-1,2-benzenediol	H	0.5	0.6	0.0	0.0
19	37.9	p-Vinyl-guaiacol	G	2.4	0.6	0.0	0.0
20	38.6	2-Methyl-6-propylphenol	H	0.0	0.0	0.0	0.0
21	40.0	Syringol	S	0.6	0.0	0.0	0.0
22	40.5	p-Isobutyl-phenol	H	0.6	0.0	0.9	0.0
23	41.0	4-Propyl-guaiacol	G	0.2	2.1	2.4	1.8
24	46.0	4-Methyl-syringol	S	0.6	0.6	0.6	0.0
25	46.5	4-(1-Propenyl)-guaiacol	G	1.2	0.0	0.0	0.0
26	56.9	4-Propyl-syringol	S	0.0	0.9	1.2	0.0
27	63.1	4-(2-propenyl)-syringol	S	0.7	0.0	0.0	0.0
28	72.3	Hexadecanoic acid	C	0.9	0.6	0.6	1.2
29	73.1	Ethyl hexadecanoate	C	0.1	1.2	1.2	1.2
		Sum of G-type lignin derivatives		7.2	5.4	5.7	3.0
		Sum of S-type lignin derivatives		1.9	1.5	1.8	0.0
		Total		**24.6**	**17.1**	**21.3**	**9.0**

[a]: C, carbohydrate derivatives; H, lignin p-hydroxyphenyl type derivatives; G, lignin guaiacyl type unit derivatives; S, lignin syringyl type derivatives

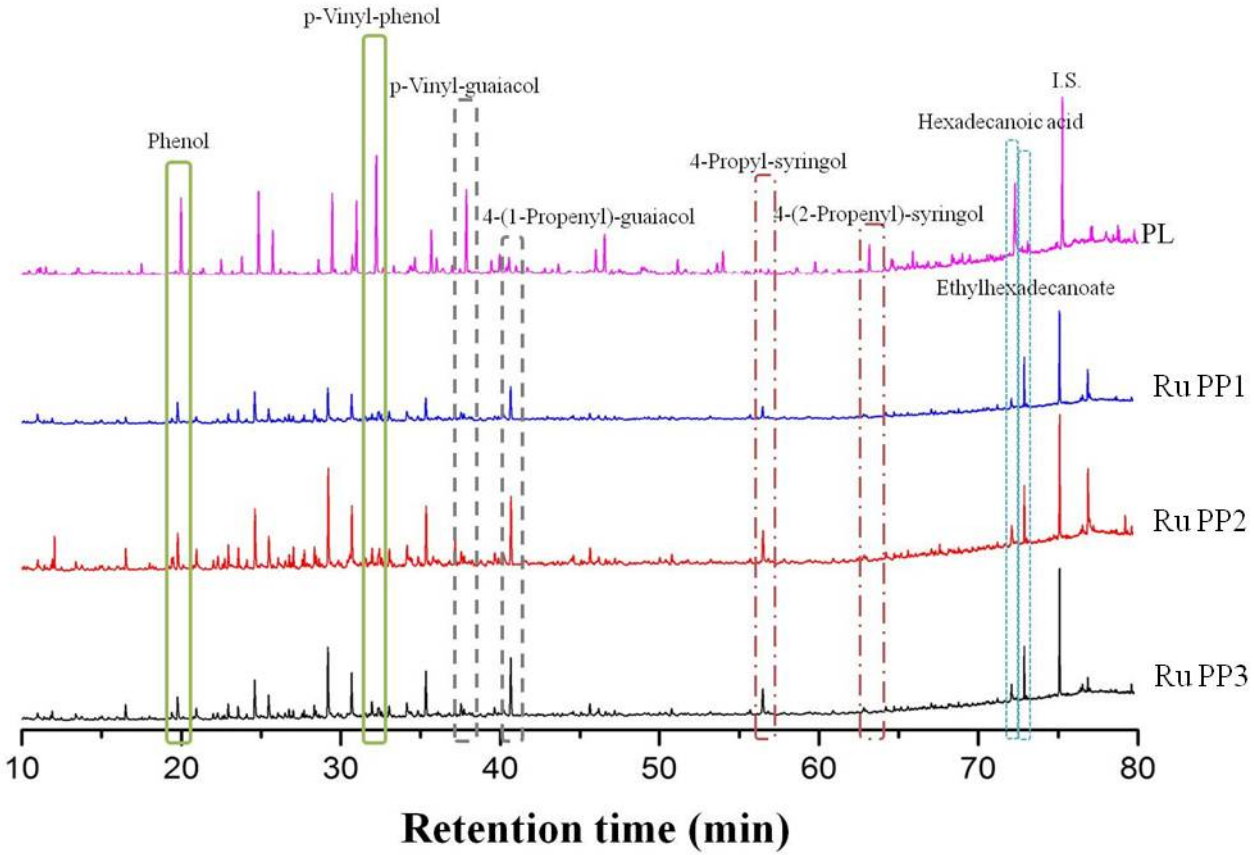

Figure 12. Gas chromatograms of lignin fragments (Ru PP1-3)

4.3. Bio-oil modifications during HDO with Pt/C catalyst

4.3.1. Mass balance of hydrodeoxygenation products

4.3.1.1. Influence of reaction temperature

The yields of HDO products obtained at 250-350°C with HDO are shown in Table 14. The product yield shows that the composition of HDO products was affected by temperature. The heavy oil yield, which ranged between 34.9-56.3% based on the weight of bio-oil, was evenly of higher value, compared with that from Pd/C and Ru/C. Additionally, the yield of heavy oils gradually increased with increasing reaction temperature up to 300°C (40.3-56.3%) then decreased when the reaction temperature increase up to 350°C. A representative example at 30 min shows that, heavy oil yield increased from 39.5% (250°C) to 56.3% (300°C) followed by a decrease to 35.3% (350°C). In contrast to heavy oil, light oil yield continuously decreased with increasing reaction temperature, typically from 32.7 (250°C) to 28.2% (350°C) at 30 min. Char yield decreased while gas yield increased with increasing reaction temperature. Especially, 6.1-8.7% char and 29.2-32.8% gas were produced at 350°C. This value of char yield was lower, and gas yield was higher than that obtained using Pd/C and Ru/C. The result indicates that the HDO level of Pt/C was at its maximum at a sustained temperature of 300°C, with accelerating further decomposition of organics over 300°C (Liu et al., 2012a).

4.3.1.2. Influence of reaction time

Reaction time, another major factor, was controlled 30, 45 and 60 min at 250, 300 and 350°C, respectively. No significant relationship between reaction time and heavy oil yield was noted during the HDO reaction with Pt/C. At the same temperature, a similar yield of heavy oil was obtained (39.5-

43.6% at 250°C; 40.3-56.3% at 300°C; 34.9-37.5% at 350°C). Light oil yield was also not related to reaction time as well as to reaction temperature. Char and gas yield tend to increase slightly with increasing reaction time, but differences were so insignificant (10.3-14.9 and 12.6-17.6% at 250°C; 6.2-11.5 and 6.5-23.5% at 300°C; 6.1-8.7% and 29.2-32.8% at 350°C, respectively).

Of the three noble metal catalysts used in these experiments (Pd/C, Ru/C and Pt/C), Pd/C was found to be most affected by both reaction temperature and reaction time. Ru/C had similar features to Pd/C but reaction temperature was a more sensitive factor than reaction time, and the relationship with reaction time was also less significant than that of Pd/C. Finally, Pt/C was only affected by reaction temperature, with effective HDO reaction at 300°C.

Table 14. The distribution of product yields as a function of reaction temperature and reaction time (wet basis, Pt/C catalyst loading: 4wt%, H_2 pressure: 30bar)

Yield (%)	Pt1	Pt2	Pt3	Pt4	Pt5	Pt6	Pt7	Pt8	Pt9
	250°C 30min	250°C 45min	250°C 60min	300°C 30min	300°C 45min	300°C 60min	350°C 30min	350°C 45min	350°C 60min
Char	10.3 (1.7)[a]	14.9 (3.2)	12.8 (0.5)	7.2 (0.4)	6.2 (0.0)	11.5 (0.4)	8.7 (1.8)	6.1 (0.0)	7.7 (0.0)
Light oil	32.7 (3.3)	29.0 (2.5)	32.2 (3.8)	30.0 (0.9)	22.7 (1.8)	26.7 (0.7)	28.2 (0.1)	26.2 (0.6)	23.7 (0.4)
Heavy oil	39.5 (1.2)	43.6 (2.9)	40.4 (3.7)	56.3 (1.5)	47.6 (1.4)	40.3 (1.1)	35.3 (4.9)	34.9 (5.5)	37.5 (5.2)
Gas	17.6 (0.6)	12.6 (2.3)	14.6 (0.6)	6.5 (1.0)	23.5 (3.2)	21.5 (0.8)	29.2 (1.3)	32.8 (4.9)	32.8 (2.5)

[a]: Standard deviation

4.3.2. Characterization of heavy oil

4.3.2.1. Physicochemical properties

Several physicochemical properties of Pt1-9, such as water content, pH, viscosity, elemental composition and higher heating value were determined, with results presented in Table 15. Water content decreased from 17.7% in bio-oil to 0.5-4.0% in Pt1-9 during the HDO reaction. If water content in Ru1-9 was affected by reaction time and that in Pd1-9 was independent of reaction conditions, water content contained in Pt1-9 was affected by reaction temperature and slightly by reaction time, especially over 45 min. As shown in Table 15, water content of Pt1-9 revealed a similar tendency to the yield of Pt1-9. Water content of Pt1-9 increased from 2.1 to 3.5% up to a reaction temperature of 300°C and then decreased to 0.8% at 350°C at 30 min.

The pH value of bio-oil (2.5) increased to 4.5-5.2 in Pt1-9, with this representing the highest pH value among heavy oils from the three noble metal catalysts. However, in the case of other oils, there was no significant relationship between pH and reaction conditions and the differences between heavy oil from the three noble metal catalysts were also minor. Viscosity decreased from 29.6 cSt for bio-oil to 2.2-6.0 cSt for Pt1-9, similar to heavy oils from other catalysts, with a narrow range between reaction conditions.

As in the case of Pd1-9 and Ru1-9, the carbon level increased from 40 wt% (bio-oil) to 45.3 (Pt2) - 70.7 (Pt8) wt% in Pt oils while oxygen level decreased from 52.2 wt% (bio-oil) to 20.1 (Pt8) – 45.4 (Pt2) wt%. It is resulted from dehydration of oxygen containing compounds as well as decrease water content. Removal of oxygenated compounds also resulted in higher HHV from 20.7 (Pt2) to 27.8 MJ/kg (Pt8) compared with bio-oil (17.3 MJ/kg). HHV of Pt8 was the highest among all of heavy oils (Pd1-9, Ru1-9 and other Pt oils).

A Van Krevelen diagram (Fig. 13) described the H/C ratio, which ranged

from 1.5-2.4 and the decrease in O/C ratio, which ranged from 0.2-0.7, compared with that of bio-oil (1.0). A decrease in O/C ratio meant that deoxygenation was effectively performed under all conditions with Pt/C. Since Pt8 had a high carbon level with low oxygen level, the O/C ratio of Pt8 decreased 5 times (0.2) compared with that of bio-oil (1.0). This indicates that the condition of Pt8 is suitable for deoxygenation. In Fig. 13, it is presumed that the reaction time Pt/C was not affected by reaction time, while it differed from reaction temperature. At 30 min, the O/C ratio decreased while the H/C ratio was maintained with increasing temperature. However, both O/C and H/C ratio decreased with increasing reaction temperature up to 350°C at 45 and 60 min. However, it is still necessary to reach an ideal O/C ratio (0.02), as discussed by Fogassy (Fogassy et al., 2011).

Table 15. Physicochemical properties of bio-oil and heavy oils (wet basis, Pt/C catalyst loading: 4wt%, H_2 pressure: 30bar)

	Bio-oil	Pt1	Pt2	Pt3	Pt4	Pt5	Pt6	Pt7	Pt8	Pt9
Water content (wt%)	17.7	2.1	4.0	3.2	3.5	3.9	1.3	0.8	0.5	0.5
pH	2.5	4.5	4.6	4.9	5.1	5.1	5.1	5.2	4.8	4.9
Viscosity (cSt)[a]	29.6	3.4	2.5	3.3	3.0	2.2	3.0	4.2	4.4	6.0
C (wt%)	40.0	55.6	45.3	51.1	53.0	47.8	56.8	59.8	70.7	67.5
H (wt%)	7.5	8.9	9.1	8.3	8.2	8.6	9.2	9.2	9.0	8.6
N (wt%)	0.2	0.0	0.0	0.0	0.1	0.0	0.0	0.0	0.2	0.1
O[b] (wt%)	52.2	35.2	45.5	40.5	38.7	43.5	33.9	30.9	20.1	23.8
S (wt%)	0.2	0.2	0.1	0.1	0.1	0.0	0.1	0.0	0.0	0.1
HHV (MJ/kg)[c]	17.3	23.5	20.7	21.8	22.3	21.0	24.0	24.8	27.8	26.6

[a]:Measured at 40°C
[b]:Calculated by difference
[c]:High heating value was calculated following formula[21],
HHV(MJ/kg) = -1.3675 + (0.3137 X C) + (0.7009 X H) + (0.0318 X O)

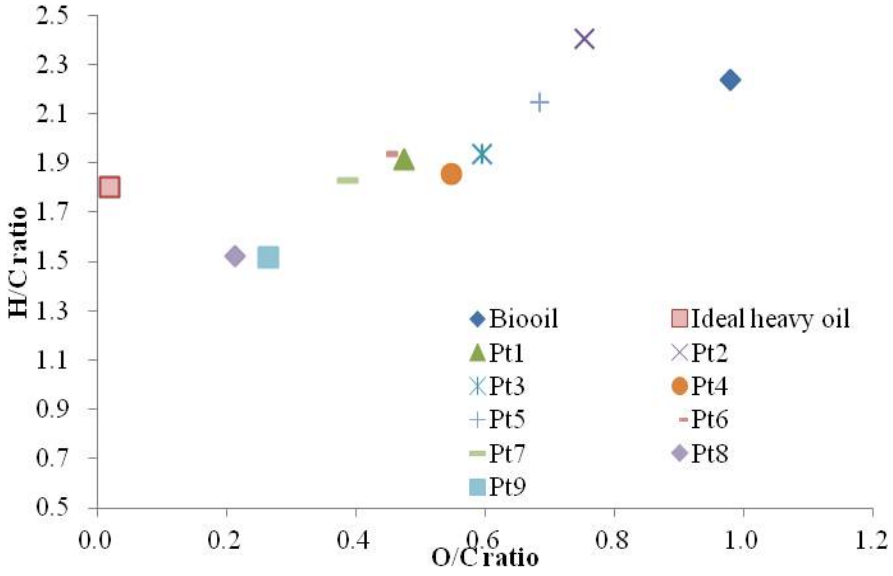

Figure 13. Van Krevelen diagram of bio-oil, heavy oils performed with Pt/C

4.3.2.2. Qualification and modification of low molecular compounds

The 32 kinds of micromolecules identified in Pt1-9 from GC/MS analysis are shown in Table 16, with their classification by functional group and distribution of their relative concentration shown in Fig. 14. Pt1-9 mainly consisted of various monomeric phenols such as guaiacol, 4-ethyl-phenol and 4-methyl-guaiacol. As shown in Fig. 14, common changes such as decreases in acids, aldehydes, sugars, alcohols and alkylbenzenes and increasing esters and phenols were investigated during the reaction. Notably, small amounts of alkylbenzenes remained in Pt1-9 and an increase in esters and phenols was detected in Pt1-9 compared with bio-oil. Moreover, Pt7-9 revealed high micromolecule concentrations compared with other Pt oils and bio-oil. Moset notably, phenols increased by ca 2 times compared with bio-oil. The gas chromatogram in Fig. 15 describes the transition in the composition of phenols. Visible peaks were phenol, 4-methyl phenol, 4-ethyl phenol, guaiacol, 4-ethyl guaiacol, 4-propyl guaiacol and syringol. These peaks were saturated and stable forms of phenols, compared with 4-vinyl phenol, 4-vinyl guaiacol and 4-(1-propenyl)-guaiacol in bio-oil (Table 16). Phenols increased from 31.4% in bio-oil to 82.5-89.9% in Pt1-9. Typically unsaturated 4-vinyl-phenol (2.4%) and 4-(1-propenyl)-guaiacol (1.6%) in bio-oil decreased while 4-ethyl-phenol (13.2-20.7%) and 4-methyl-guaiacol (8.8-17.2%) increased and phenol (6.8-11.3%), 2-methyl-phenol (3.6-5.8%) and 4-methyl-phenol (4.4-11.3%), which were not identified in bio-oil, were found in Pt1-9. These were products of HDO via demethoxylation, demethylation hydrogenation, dealkylation and ring opening.

Meanwhile, 2-methyl-benzofuran (4.1%) in bio-oil also decreased to 0.7-1.3%, and 3.5-6.8% of 2-methyl-phenol was formed in heavy oils. This could be the result of dealkylation via ring opening (Furimsky, 2000; Liu et al., 2012b). Considering that 2-propyl-phenol was originally presented in bio-oil (2.4%) and that an expected intermediate of the above reaction remained in Pt1-9 (1.1-3.7%), ring opening of furan progressed and coincided with further dealkylation of 2-methyl-phenol. In addition, 2-propyl phenol (1.1-3.7%) and 4-propyl-guaiacol (6.3-7.8%) were detected at levels lower than those in Pd1-9 (2.3-11.0% and 5.4-8.4%, respectively), while 4-methyl phenol (4.4-11.3%), 4-methyl guaiacol (8.8-17.2%) and 4-ethyl guaiacol (8.3-11.8%) were detected at levels higher than those in Pd1-9 (2.3-13.2%, 6.1-9.7% and 7.9-11.8%, respectively), especially at 350°C. Therefore, Pt/C is good at dealkylation, which is also evidence of further decomposition at high temperatures.

Evidently, unstable and undesired compounds such as 2-hydroxy-butanoic acid (4.5%), furfural (11.7%), levoglucosan (18.9%) and butandial (1.8%) in bio-oil were removed and relatively stable esters such as 4-oxo-pentanoic acid ethyl ester or ketones, 2-methyl-cyclopentanone (0.5-5.7%), 2-ethyl-cyclopentanone (1.0-7.8%) and 2,5-hexadione (0.9-2.8%) increased in Pt1-9. This was due to hydrogenation, decarbonylation, dehydroxylation and ring opening. Thus, the formation of esters, which are produced by hydrogenation, dehydroxylation and decarbonylation during the HDO of bio-oil, could be derived from furfural and levoglucosan, but not from an aromatic ring (Sitthisa & Resasco, 2011). Although the types of reaction taking place during HDO were similar, there were differences for each noble metal catalyst (Pd/C, Ru/C and Pt/C).

Table 16. Quantitative analysis of low molecular weight components in bio-oil and heavy oil (wet basis, Pt /C catalyst loading: 4wt%, H_2 pressure: 30bar)

	Compound	Relative area(peak area/ I.S. area)									
		Bio-oil	Pt1	Pt2	Pt3	Pt4	Pt5	Pt6	Pt7	Pt8	Pt9
	Acids										
1	Butanoic acid, 2-hydroxy-	0.5 (4.5)	-	-	-	-	-	-	-	-	-
	Phenols										
2	Phenol	-	1.0 (7.8)	0.8 (8.1)	0.9 (7.6)	0.7 (7.4)	0.8 (6.8)	1.1 (8.4)	1.4 (9.4)	2.2 (9.8)	2.1 (11.3)
3	2-Methyl-phenol	-	0.5 (3.6)	0.4 (3.7)	0.6 (5.2)	0.5 (5.4)	0.4 (3.5)	0.5 (3.8)	0.7 (4.7)	1.5 (6.8)	1.0 (5.8)
4	4-Methyl-phenol	-	0.6 (4.9)	0.5 (5.1)	0.5 (4.4)	0.5 (4.8)	0.5 (4.4)	0.7 (5.6)	1.4 (9.1)	2.4 (10.9)	2.0 (11.3)
5	Guaiacol	0.9 (8.1)	1.5 (11.4)	1.2 (11.8)	1.4 (11.7)	1.2 (12.1)	1.4 (11.8)	1.5 (12.0)	1.6 (10.2)	1.6 (7.4)	1.0 (5.8)
6	2,4-Dimethyl-phenol	-	0.2 (1.7)	0.2 (1.8)	0.2 (1.6)	0.2 (1.6)	0.2 (1.7)	0.2 (1.9)	0.3 (2.2)	0.1 (0.6)	0.1 (0.5)
7	4-Ethyl-phenol	0.3 (2.7)	1.7 (13.2)	1.4 (13.7)	1.7 (14.4)	1.6 (15.4)	2.1 (17.1)	2.1 (16.5)	2.5 (16.4)	4.6 (20.7)	3.5 (19.4)
8	2,3-Dimethyl-phenol	0.3 (2.7)	0.1 (.8)	0.1 (0.8)	0.1 (0.7)	0.1 (1.0)	0.1 (1.0)	0.2 (1.4)	0.2 (1.5)	0.5 (2.3)	0.5 (2.6)
9	4-Methyl-guaiacol	0.3 (2.7)	2.2 (16.6)	1.7 (17.2)	1.5 (12.6)	1.2 (12.3)	1.3 (10.5)	1.4 (10.8)	1.4 (9.2)	1.9 (8.8)	1.8 (10.1)
10	4-Vinyl-phenol	0.3 (2.7)	-	-	-	-	-	-	-	-	-
11	2-Propyl-phenol	0.3 (2.7)	0.2 (1.6)	0.2 (1.7)	0.1 (1.1)	0.1 (1.1)	0.2 (1.3)	0.2 (1.6)	0.3 (2.0)	0.8 (3.4)	0.7 (3.7)
12	4-Ethyl-guaiacol	0.2 (1.8)	1.1 (8.3)	0.9 (8.6)	1.1 (9.6)	1.2 (11.5)	1.4 (11.8)	1.4 (11.1)	1.5 (9.8)	1.9 (8.6)	1.7 (9.1)
13	Syringol	0.2 (1.8)	1.0 (7.7)	0.8 (8.0)	0.8 (6.9)	0.7 (6.6)	0.7 (5.8)	0.8 (6.2)	0.6 (4.1)	0.8 (3.7)	0.6 (3.4)
14	4-Propyl-guaiacol	0.6 (5.4)	0.8 (6.3)	0.7 (6.5)	0.8 (6.7)	0.8 (7.5)	1.0 (7.8)	1.0 (7.6)	1.0 (6.7)	1.4 (6.6)	1.3 (6.9)
15	4-Methyl-syringol	0.1 (0.9)	-	-	-	-	-	-	-	-	-
16	4-(1-Propenyl)-guaiacol	0.2 (1.8)	-	-	-	-	-	-	-	-	-
	Aldehydes										
17	Furfural	1.3 (11.7)	-	-	-	-	-	-	-	-	-
	Sugars										
18	Levoglucosan	2.1 (18.9)	-	-	-	-	-	-	-	-	-
	Esters										
19	Pentanoic acid, 4-oxo-, ethyl ester	-	0.5 (4.0)	0.4 (4.2)	0.3 (2.8)	0.2 (2.1)	0.2 (1.7)	0.2 (1.3)	0.2 (1.4)	0.2 (0.7)	0.1 (0.5)
20	Hexadecanoic acid, ethyl ester	-	-	-	-	-	-	-	-	-	-
21	Octadecanoic acid, ethyl ester	-	-	-	-	-	-	-	-	-	-
	Alcohols										
22	Butanedial	0.2 (1.8)	-	-	-	-	-	-	-	-	-
	Ketone										
23	2-Methyl-cyclopentanone	-	0.5 (4.1)	0.3 (2.7)	0.7 (5.7)	0.1 (1.2)	0.2 (1.4)	0.1 (0.9)	0.5 (3.3)	0.1 (0.5)	0.1 (0.5)
24	2-Ethyl-cyclopentanone	-	0.3 (2.0)	0.1 (1.0)	0.3 (2.9)	0.5 (5.3)	1.0 (7.8)	0.9 (6.8)	0.9 (6.2)	1.4 (6.4)	1.2 (6.4)
25	2,5-Hexanedione	-	0.3 (2.5)	0.1 (1.2)	0.3 (2.6)	0.2 (2.2)	0.3 (2.8)	0.2 (1.2)	-	0.2 (0.9)	0.2 (1.0)
26	2-Ethyl-2-cyclopentenone	0.4 (3.6)	-	-	-	-	-	-	-	-	-
27	2,3-Dimethyl-2-cyclopentenone	0.4 (3.6)	0.4 (2.8)	0.3 (2.9)	0.3 (2.7)	0.2 (1.9)	0.2 (1.7)	0.2 (1.9)	0.4 (2.5)	0.1 (0.6)	0.1 (0.6)
28	4-Hydroxy-5,6-dihydro-(2H)-pyranone	0.3 (2.7)	-	-	-	-	-	-	-	-	-
29	2-Hydroxy-3-methyl-2-cyclopentenone	0.4 (3.6)	-	-	-	-	-	-	-	-	-
	Alkylbenzenes										
30	1,3-Dimethyl- benzene	1.3 (11.7)	-	-	-	-	-	-	-	-	-
31	1,2,3-trimethoxy-5-methyl -benzene	-	-	-	-	-	-	-	-	-	-
32	2-Methyl- benzofuran	0.5 (4.5)	0.1 (1.0)	0.1 (1.0)	0.1 (0.7)	0.1 (0.7)	0.2 (1.3)	0.1 (0.8)	0.1 (0.9)	0.3 (1.3)	0.2 (1.2)
	Total	11.1	13.1	10.5	11.9	10.1	12.2	12.6	15.2	22.1	18.2

[a]: plausible portion of each compound in oil

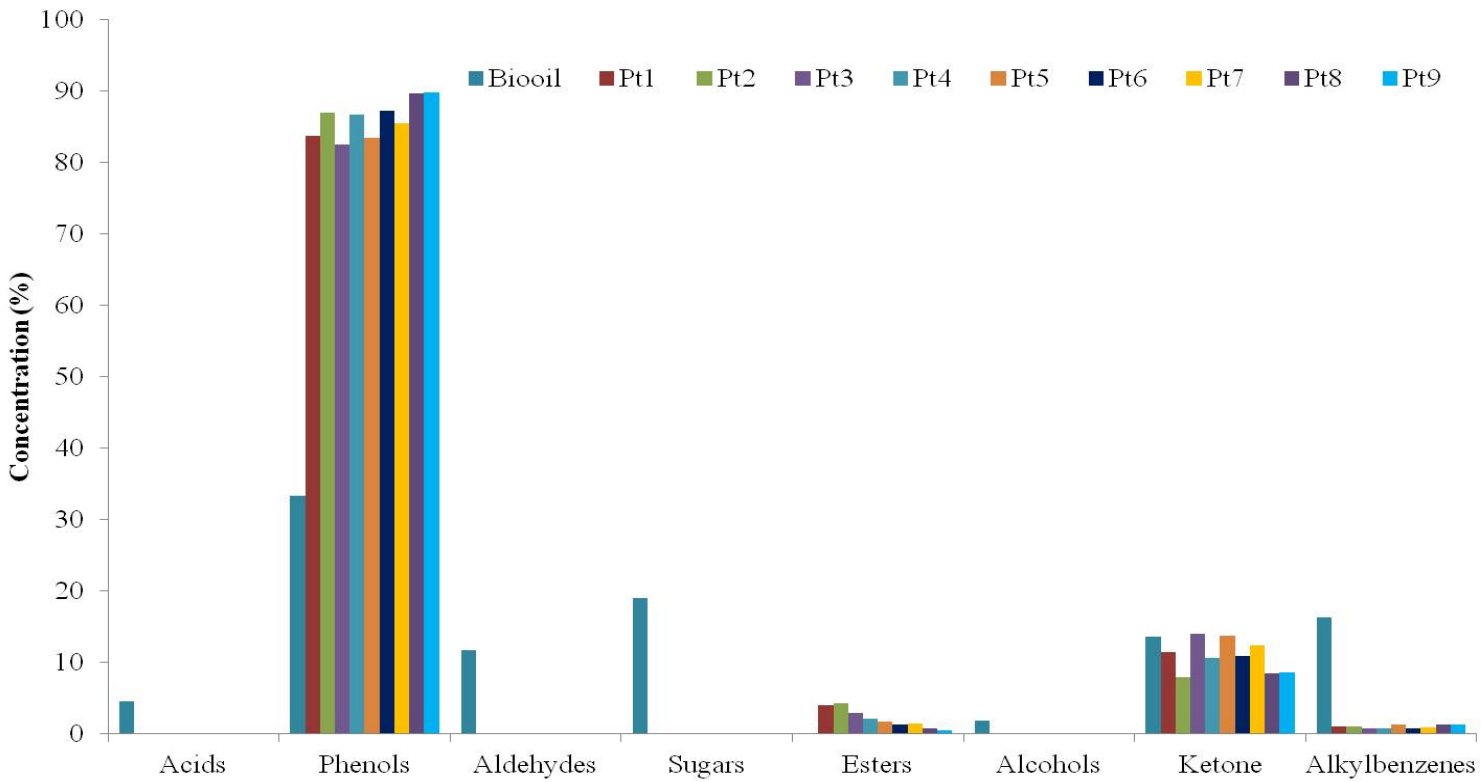

Figure 14. Distribution of compounds in heavy oil performed with Pt/C at 45 min (Reaction temperature: 250, 300 and 350°C, Catalyst: 4 wt%, Ethanol/bio-oil ratio: 1/4 (w/w), H_2 pressure: 30 bar)

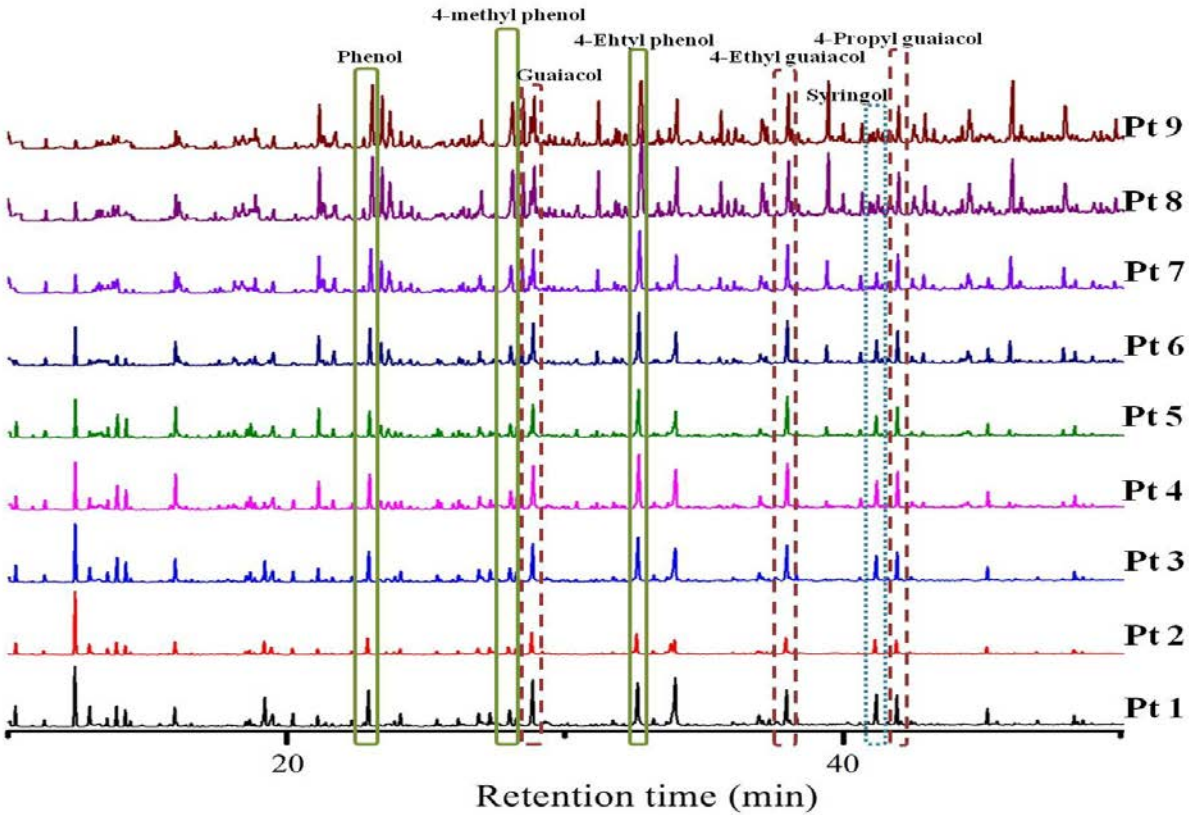

Figure 15. Gas chromatogram of Pt1-9

4.3.3. Macromolecular transitions from bio-oil to heavy oil

4.3.3.1. Physicochemical properties

As in the case of macromolecule extraction from Pd and Ru oils, Pt4-6 were selected to extract phenol polymers (Pt PP1-3). Typical chemical properties were then measured, with results presented in Table 17. Yields of Pt PP1-3 based on the weight of bio-oil decreased notably from 22.4% (PL) to 3.5-6.5%, comprising 15.6-29.0% of PL, respectively. A previous study showed that a HDO reaction with supercritical ethanol effectively converted macromolecules, which resulted in improved heavy oil properties (Tang et al., 2010). In addition, Pt/C accelerates further decomposition, also effectively resulting in macromolecule conversion (Xu et al., 2012). The significant decreasing trend of Pt PP1-3 compared with PL was indirect evidence that bio-oil improved stability through the HDO reaction.

The carbon level increased from 65.0 wt% (PL) to 75.2-76.8 wt% (Pt PP1-3). However, the oxygen content of Pt PP1-3 decreased to 15.5-18.0 wt%, compared with that of PL (27.8 wt%). Major functional groups of lignin derived phenols, both phenolic hydroxyl and methoxyl groups, decreased from 6.8 and 11.6% in PL to 2.0-2.1 and 0.1-1.0% in Pt PP1-3, respectively. Methoxyl groups decreased notably with increasing reaction time and decreased to a similar level with other phenol polymers (Pd PP1-3 and Ru PP1-3). Phenolic hydroxyl groups decreased to the greatest degree, Pd PP1-3 (4.0-5.1%), Ru PP1-3 (5.0-6.1%) and Pt PP1-3 (2.0-2.1%). This suggested that demethoxylation was one of the major reactions of deoxygenation and easily occurred with Pt/C, with inducing linked or dehydroxylated phenolic hydroxyl groups.

Table 17. Characteristics of lignin fragment extracted from Pt4-6

Lignin fragment	Yield (%)	Elemental analysis (wt%)				Average molecular Weight			Functional groups (%)	
		C	H	N	O	M_w (Da)	M_n (Da)	PDI(M_w/M_n)	Phe-OH	OCH_3
PL	22.4	65.0	6.4	0.6	27.8	1,065	544	2.0	6.8(0.6)[e]	11.6(1.1)
Pt PP1 [b]	3.5(9.5) [a]	75.2	6.7	0.2	18.0	827	560	1.5	2.1(0.5)	1.0(0.4)
Pt PP2 [c]	5.9(12.4)	75.6	7.9	0.0	16.5	818	576	1.4	2.2(0.2)	0.2(0.0)
Pt PP3 [d]	6.5(17.2)	76.8	7.8	0.0	15.5	783	541	1.4	2.0(0.9)	0.1(0.0)

[a]: Based on the weight of crude oil.
[b]: phenol polymer obtained from Pt 4
[c]: phenol polymer obtained from Pt 5
[d]: phenol polymer obtained from Pt 6
[e]: standard deviation

4.4. Recovery and reuse of noble metal catalysts for HDO reactions

4.4.1. Mass balance of HDO products with reused catalysts and heavy oil properties

Each catalyst was recovered from the char-catalyst mixture. HDO was then performed with recovered catalysts at 300°C for 45min. Recycling of catalysts was carried out three times. The yield of each product obtained from the reused catalyst is described in Fig. 16. HDO with the reused three noble metal catalysts showed that heavy oil yield diminished with each reuse experiment. Pd/C yielded 41.6% heavy oil in its fresh state, but the yield of heavy oil decreased to 33.3-25.2% with three recycling efforts. The 38.2% heavy oil obtained from fresh Ru/C also decreased to 35.9-20.8% after recycling. Similarly, Pt/C was deprived of its HDO degree with recycling. It produced 47.6% of heavy oil at first use, but this decreased to between 44.7-24.9% with reuse. The trend was due to the deactivation of catalysts, especially through deposited char and poisoning of active sites (Kushiyama et al., 1990). It also led to an increase in char yield. This could be due to the reduction of efficient collision between organics in liquid bio-oil and catalyst active sites. The yield of char increased from 5.5 to 23.6% (Pd/C), to 10.4-29.7% (Ru/C) and to 6.2-26.7% (Pt/C) with increasing recycling number. In previous study, remaining or produced char was deactivated catalyst. Since active sites were covered by char, coke formation accelerated and char yield consequentially increased (Fisk et al., 2009).

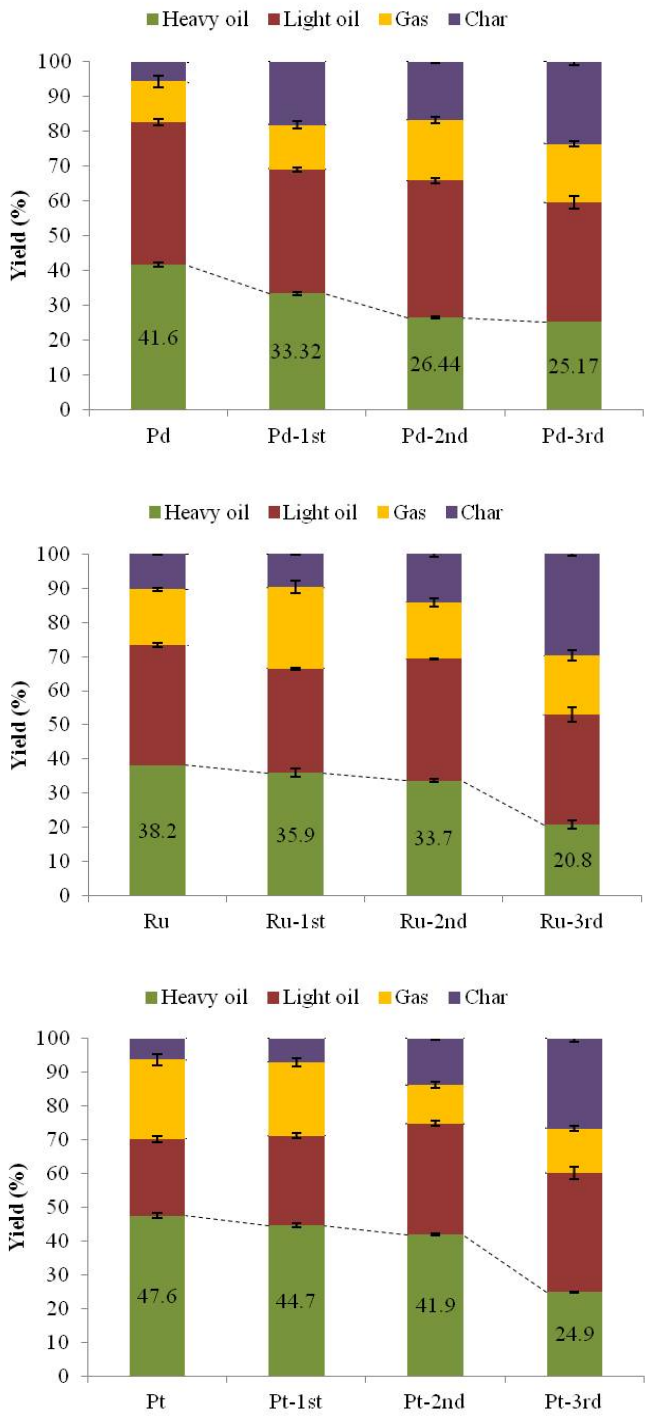

Figure 16. Mass balance of HDO reaction with fresh and reused catalysts (300℃, 45 min, H_2: 30 bar)

Table 18. Physicochemical features of heavy oils obtained from reused noble metal catalysts

	Pd-1st	Pd-2nd	Pd-3rd	Ru-1st	Ru-2nd	Ru-3rd	Pt-1st	Pt-2nd	Pt-3rd
Water content (wt%)	2.2 (0.1)	3.0 (0.1)	7.4 (0.3)	2.4 (0.1)	5.0 (0.1)	5.6 (0.2)	3.9 (0.0)	3.9 (0.4)	4.2 (0.0)
pH	4.6 (0.0)	4.6 (0.0)	4.6 (0.0)	4.7 (0.0)	4.1 (0.0)	3.9 (0.0)	4.4 (0.0)	4.7 (0.0)	4.6 (0.1)
M_w (Da)	930	928	945	923	929	1022	829	830	834
M_n (Da)	506	589	607	519	540	567	497	490	508
PDI[a]	1.8	1.6	1.6	1.8	1.7	1.8	1.7	1.7	1.6
C (wt%)	67.8	60.9	56.9	65.0	59.9	53.7	62.1	57.1	38.7
H (wt%)	7.3	7.9	7.5	7.7	6.9	7.5	7.9	8.0	5.7
N (wt%)	0.5	0.3	0.3	0.4	0.3	0.3	0.4	0.3	0.2
O[b] (wt%)	24.4	30.9	35.3	26.9	32.8	38.5	29.5	34.6	55.3
S (wt%)	0.0	0.0	0.0	0.0	0.1	0.1	0.1	0.1	0.1
HHV(MJ/kg)[c]	25.0	23.3	21.8	24.4	22.2	20.7	24.6	23.2	16.5

[a]: Polydispersity index(PDI) means the value of M_w/M_n
[b]: Calculated by difference
[c]: High heating value was calculated following formula,
HHV(MJ/kg) = -1.3675 + (0.3137 X C) + (0.7009 X H) + (0.0318 X O)

4.4.2. Deactivation degree of each noble metal catalyst with reuse

Since catalysts were deactivated by coke deposition and destroy by repeated experiments, the yield of heavy oil decreased and heavy oil properties also changed compared with the heavy oil obtained from fresh catalysts. The deactivation degree of catalysts could be elucidated, and the expected deactivation mechanism of catalysts was investigated. It was assumed that only coke deposition influenced catalyst deactivation and that char was deposited on the active site at a ratio of 1:1 (w/w); total deactivation degree (Fig. 17) was calculated based on the ratio between weight gain after recovery and original weight of catalyst.

As described in Fig. 17, Pd/C deactivated only by 0.5% with use in its fresh state. However, deactivated decreased sharply to 37.6% after the first recycle, with total deactivation of 42.9% after two cycle of use. Ru/C showed a different trend compared with Pd/C. Its deactivation degree was proportional to the use cycle, at 25.6, 33.4 and 36.8% after each experiment. From among the three catalysts, Pt/C could best endure repeated recycling experiments (15.7% after first use; 16.8% after first recycling experiment; 56.7% after second recycling), elucidated on the basis of higher heat resistance of Pt compared with Pd and Ru (Albers et al., 2001). However, it deactivated the most at the end of the three experiments. Among the 5 causes of catalyst deactivation mentioned above, coke deposition was reasonably assumed to apply for the HDO reaction with metal catalysts supported on activated carbon. Aromatic ring condensation products acted as a coke precursor (Mao et al., 2013), which deposited on the catalyst and deactivated its activity. As shown in Tables 4, 11 and 16, GC/MS detectable phenol compounds decreased in sequence of Pd, Pt and Ru. Total catalyst

deactivation degree (Fig. 17) showed the same tendency in terms of decreased amounts of phenol compounds in heavy oils. Results indicate that coke formation originating from lignin derived phenols was a main factor in deactivation of noble metal catalysts supported on activated carbon. However, the total deactivation degree was measured after removal of physically deposited coke. Therefore, the coke originating from lignin derived phenols might deactivate the catalyst by poisoning (Kushiyama et al., 1990).

Slight degree of poisoning by sulfur (Fig. 18) were also expected to occur during HDO with Ru/C and Pt/C. Sulfided CoMo/NiMo, widely used in HDO, have been shown to be able to partially eliminate sulfur compounds. This was expected from a decrease bio-oil sulfur level from 0.2 to 0.0-0.1% after HDO with Ru/C and Pt/C (Tables 10 and 15).

In addition, there were unusual deactivation mechanisms during hydrogenation; dealkylated CH_3 combined with noble metal surface such as Metal-CH_3 form. Sulfur poisoning and Metal-CH_3 formations might reduce the number of efficient collision between catalysts active sites and substance (organics in heavy oil). The form could reduce hydrogen storage and release grade and also decrease catalytic reactivity (Albers et al., 2001).

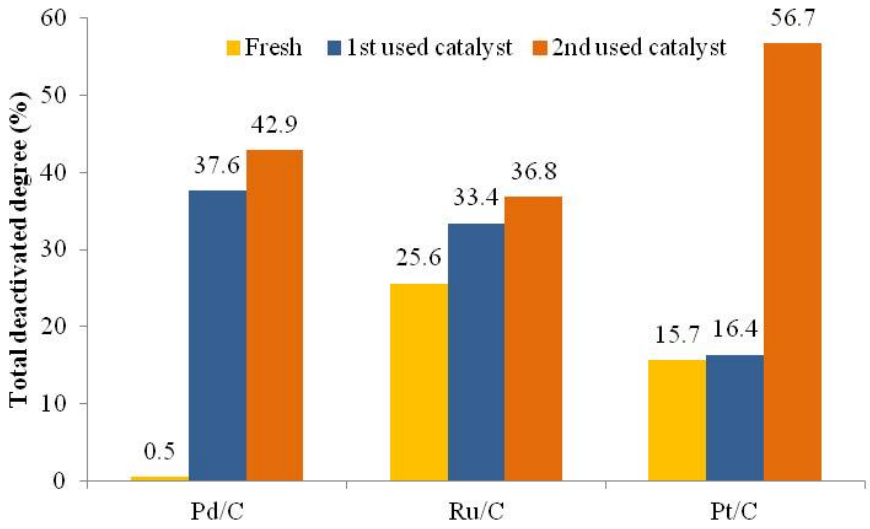

Figure 17. Deactivation degree based on fresh catalyst with increasing reuse cycle

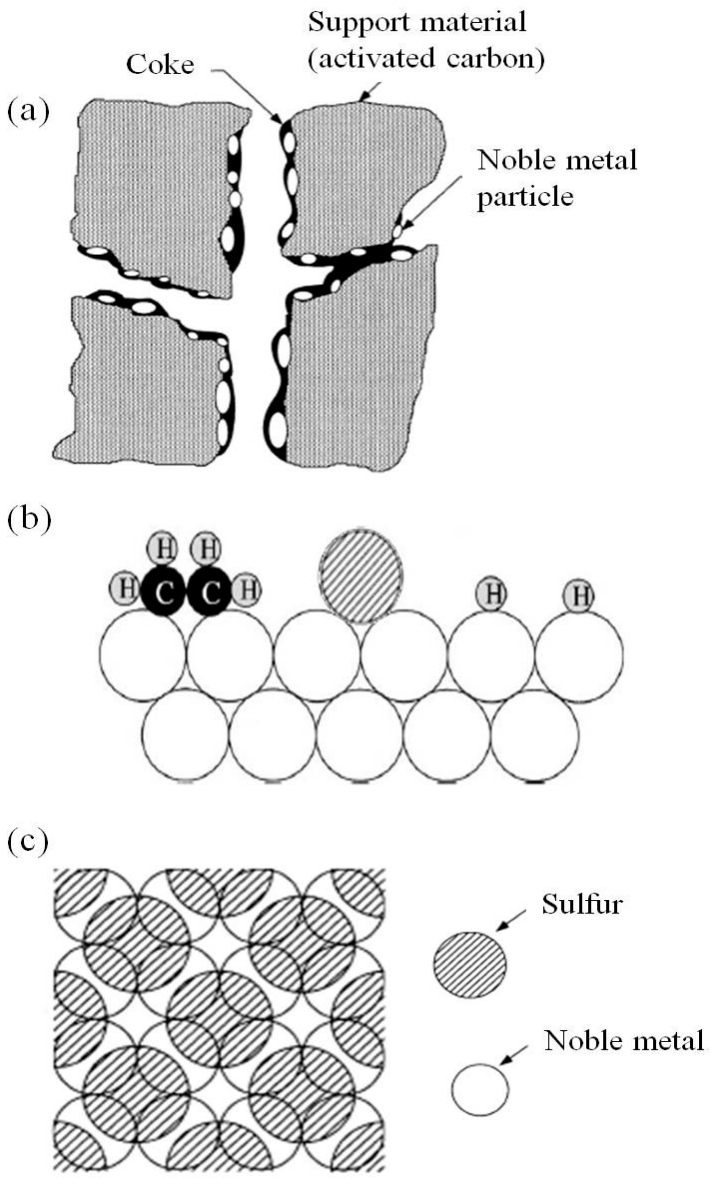

Figure 18. Expected mechanism of deactivation of noble metal catalysts; (a) coke deposition; (b) sulfur poisoning during hydrogenation; (c) illustration of sulfur adsorbed on noble metal layer (Bartholomew, 2001)

5. Conclusion

This study investigated the effect of process conditions and of different types of catalyst on hydrodeoxygenation (HDO) products, and on improvement of fuel properties, structural features and stability. Gas, char and two phase oil (light and heavy oil) were produced after conducting HDO of miscanthus bio-oil. The yield of each product indicated that HDO was significantly affected by reaction temperature (Pd/C, Ru/C and Pt/C) and by reaction time (to a small degree with Pd/C and to a very large degree with Ru/C). When reaction conditions changed, the yield of char and gas varied together with that of heavy oil, due to polymerization and further decomposition, as well as due to HDO reactions. Physicochemical properties of heavy oils, such as water content, viscosity, acidity, carbon content and HHV, improved following HDO when compared with bio-oil, with differences in such properties depending on reaction temperature, time, as well as on reaction catalysts. Heavy oils also showed well-deoxygenated properties with lower O/C ratios than those of bio-oil, and with clear removal of undesired compounds through various reactions (e.g. hydrogenation, dealkylation, demethoxylation, ring opening, decarbonylation and dehydroxylation). Dehydration of oxygenated compounds, side chain saturation and ring opening of carbohydrate derived compounds could enhance the stability of heavy oil. Since each catalyst catalyzed different reactions during HDO, deactivation of Pd/C, Ru/C and Pt/C progressed through various mechanisms at different levels. Pd/C was especially good at hydrogenation while Ru/C was suitable for deoxygenation. Pt/C could undertake both hydrogenation and deoxygenation at proper levels.

Compared to bio-oil, heavy oils consist of relatively low amounts of phenol polymers. In addition, thermal and structural features suggest that macromolecules could be further modified to be condensed as well as stabilized during HDO reactions by hydrogenation and deoxygenation as well as through other simultaneous reactions.

Catalyst deactivation of Pd/C, Ru/C and Pt/C progressed during HDO with differences in deactivation levels commonly related to coke deposition. From amongst the three catalysts, Pt/C was the most resistant to varied circumstances and fresh state Pd/C coped with coke deposition and destruction on active sites. Ru/C was proportionately deactivated by coke deposition.

6. References

Al-Sabawi, M., Chen, J. 2012. Hydroprocessing of Biomass-Derived Oils and Their Blends with Petroleum Feedstocks: A Review. Energy & Fuels, 26(9), 5373-5399.

Albers, P., Pietsch, J., Parker, S.F. 2001. Poisoning and deactivation of palladium catalysts. Journal of Molecular Catalysis A: Chemical, 173(1), 275-286.

Ardiyanti, A., Gutierrez, A., Honkela, M., Krause, A., Heeres, H. 2011. Hydrotreatment of wood-based pyrolysis oil using zirconia-supported mono-and bimetallic (Pt, Pd, Rh) catalysts. Applied Catalysis A: General, 407(1), 56-66.

Argyropoulos, D.S., Sun, Y. 1996. Photochemically Induced Solid -State Degradation, Condensation, and Rearrangement Reactions in Lignin Model Compounds and Milled Wood Lignin. Photochemistry and photobiology, 64(3), 510-517.

Auer, E., Freund, A., Pietsch, J., Tacke, T. 1998. Carbons as supports for industrial precious metal catalysts. Applied Catalysis A: General, 173(2), 259-271.

Baker, S. 1996. Rapid methoxyl analysis of lignins using gas chromatography. Holzforschung, 50(6), 573-574.

Bartholomew, C.H. 2001. Mechanisms of catalyst deactivation. Applied Catalysis A: General, 212(1), 17-60.

Bayerbach, R., Meier, D. 2009. Characterization of the water-insoluble fraction from fast pyrolysis liquids (pyrolytic lignin). Part IV: Structure elucidation of oligomeric molecules. Journal of Analytical and Applied Pyrolysis, 85(1), 98-107.

Boateng, A., Weimer, P., Jung, H., Lamb, J. 2008. Response of Thermochemical and Biochemical Conversion Processes to Lignin Concentration in Alfalfa Stems†. Energy & fuels, 22(4), 2810-2815.

Bok, J.P., Choi, H.S., Choi, J.W., Choi, Y.S. 2013. Fast pyrolysis of *Miscanthus sinensis* in fluidized bed reactors: Characteristics of product yields and biocrude oil quality. Energy, 60, 44-52.

Bridgewater, A.V. 2004. Biomass fast pyrolysis. Thermal Science, 8(2), 21-50.

Bridgwater, A.V. 2012. Review of fast pyrolysis of biomass and product upgrading. biomass and bioenergy, 38, 68-94.

Brown, R.C. 2003. Biorenewable resources. Iowa State Press.

Bui, V.N., Laurenti, D., Afanasiev, P., Geantet, C. 2011. Hydrodeoxygenation of guaiacol with CoMo catalysts. Part I: Promoting effect of cobalt on HDO selectivity and activity. Applied Catalysis B: Environmental, 101(3), 239-245.

Bykova, M., Zavarukhin, S., Trusov, L., Yakovlev, V. 2013. Guaiacol hydrodeoxygenation kinetics with catalyst deactivation taken into consideration. Kinetics and Catalysis, 54(1), 40-48.

Czernik, S., Bridgwater, A. 2004. Overview of applications of biomass fast pyrolysis oil. Energy & Fuels, 18(2), 590-598.

de Miguel Mercader, F., Groeneveld, M.J., Kersten, S.R., Geantet, C., Toussaint, G., Way, N.W., Schaverien, C.J., Hogendoorn, K.J. 2011. Hydrodeoxygenation of pyrolysis oil fractions: process understanding and quality assessment through co-processing in refinery units. Energy & Environmental Science, 4(3), 985-997.

Fahmi, R., Bridgwater, A., Thain, S., Donnison, I., Morris, P., Yates, N. 2007. Prediction of Klason lignin and lignin thermal degradation products by

Py–GC/MS in a collection of *Lolium* and *Festuca* grasses. Journal of analytical and applied pyrolysis, 80(1), 16-23.

Faix, O., Fortmann, I., Bremer, J., Meier, D. 1991. Thermal degradation products of wood. European Journal of Wood and Wood Products, 49(5), 213-219.

Faix, O., Meier, D., Fortmann, I. 1990. Thermal degradation products of wood. European Journal of Wood and Wood Products, 48(7), 281-285.

Fisk, C.A., Morgan, T., Ji, Y., Crocker, M., Crofcheck, C., Lewis, S.A. 2009. Bio-oil upgrading over platinum catalysts using *in situ* generated hydrogen. Applied Catalysis A: General, 358(2), 150-156.

Fogassy, G., Lorentz, C., Toussaint, G., Thegarid, N., Schuurman, Y., Mirodatos, C. 2011. Analytical techniques tailored for biomass transformation to biofuels. Environmental progress & sustainable energy.

Furimsky, E. 2000. Catalytic hydrodeoxygenation. Applied Catalysis A: General, 199(2), 147-190.

Furimsky, E., Mikhlin, J., Jones, D., Adley, T., Baikowitz, H. 1986. On the mechanism of hydrodeoxygenation of ortho substituted phenols. The Canadian Journal of Chemical Engineering, 64(6), 982-985.

Gray, K.A., Zhao, L., Emptage, M. 2006. Bioethanol. Current opinion in chemical biology, 10(2), 141-146.

Gutierrez, A., Kaila, R., Honkela, M., Slioor, R., Krause, A. 2009. Hydrodeoxygenation of guaiacol on noble metal catalysts. Catalysis Today, 147(3), 239-246.

Huber, G.W., Iborra, S., Corma, A. 2006. Synthesis of transportation fuels from biomass: chemistry, catalysts, and engineering. Chemical reviews, 106(9), 4044-4098.

Iiyama, K., Lam, T.B.T. 2006. Lignin in wheat internodes. Part 1: The reactivities of lignin units during alkaline nitrobenzene oxidation. Journal of the Science of Food and Agriculture, 51(4), 481-491.

Joshi, N., Lawal, A. 2012. Hydrodeoxygenation of pyrolysis oil in a microreactor. Chemical Engineering Science, 74, 1-8.

Kim, T.S., Kim, J.Y., Kim, K.H., Lee, S., Choi, D., Choi, I.G., Choi, J.W. 2012. The effect of storage duration on bio-oil properties. Journal of Analytical and Applied Pyrolysis.

Kushiyama, S., Aizawa, R., Kobayashi, S., Koinuma, Y., Uemasu, I., Ohuchi, H. 1990. Effect of addition of sulphur and phosphorus on heavy oil hydrotreatment with dispersed molybdenum-based catalysts. Applied catalysis, 63(1), 279-292.

Lee, J. 1997. Biological conversion of lignocellulosic biomass to ethanol. Journal of biotechnology, 56(1), 1-24.

Lee, M.-K., Tsai, W.-T., Tsai, Y.-L., Lin, S.-H. 2010. Pyrolysis of napier grass in an induction-heating reactor. Journal of Analytical and Applied Pyrolysis, 88(2), 110-116.

Lin, S.Y., Dence, C.W. 1992. Methods in lignin chemistry. Springer.

Liu, C., Shao, Z., Xiao, Z., Liang, C. 2012a. Hydrodeoxygenation of benzofuran over activated carbon supported Pt, Pd, and Pt–Pd catalysts. Reaction Kinetics, Mechanisms and Catalysis, 107(2), 393-404.

Liu, C., Shao, Z., Xiao, Z., Williams, C.T., Liang, C. 2012b. Hydrodeoxygenation of Benzofuran over Silica–Alumina-Supported Pt, Pd, and Pt–Pd Catalysts. Energy & Fuels, 26(7), 4205-4211.

Lysen, E. 2000. Global Restrictions of biomass availability for import to the Netherlands. Novem. Utrecht.

Månsson, P. 1983. Quantitative determination of phenolic and total hydroxyl groups in lignins. Holzforschung-International Journal of the Biology, Chemistry, Physics and Technology of Wood, 37(3), 143-146.

Mao, A., Wang, H., Pan, R. 2013. Coke deactivation of activated carbon-supported rubidium-potassium catalyst for C_2F_5I gas-phase synthesis. Journal of Fluorine Chemistry.

Martínez-Palou, R., Mosqueira, M.L., Zapata-Rendón, B., Mar-Juárez, E., Bernal-Huicochea, C., de la Cruz Clavel-López, J., Aburto, J. 2011. Transportation of heavy and extra-heavy crude oil by pipeline: A review. Journal of Petroleum Science and Engineering, 75(3), 274-282.

Meier, D., van de Beld, B., Bridgwater, A.V., Elliott, D.C., Oasmaa, A., Preto, F. 2013. State-of-the-art of fast pyrolysis in IEA bioenergy member countries. Renewable and Sustainable Energy Reviews, 20, 619-641.

Miao, S., Shanks, B.H. 2009. Esterification of biomass pyrolysis model acids over sulfonic acid-functionalized mesoporous silicas. Applied Catalysis A: General, 359(1), 113-120.

Mohan, D., Pittman, C.U., Steele, P.H. 2006. Pyrolysis of wood/biomass for bio-oil: a critical review. Energy & Fuels, 20(3), 848-889.

Nimmanwudipong, T., Runnebaum, R.C., Block, D.E., Gates, B.C. 2011. Catalytic reactions of guaiacol: reaction network and evidence of oxygen removal in reactions with hydrogen. Catalysis letters, 141(6), 779-783.

Oasmaa, A., Czernik, S. 1999. Fuel oil quality of biomass pyrolysis oils state of the art for the end users. Energy & Fuels, 13(4), 914-921.

Oasmaa, A., Kuoppala, E., Selin, J.-F., Gust, S., Solantausta, Y. 2004. Fast pyrolysis of forestry residue and pine. 4. Improvement of the product quality by solvent addition. Energy & Fuels, 18(5), 1578-1583.

Ohta, H., Kobayashi, H., Hara, K., Fukuoka, A. 2011. Hydrodeoxygenation of phenols as lignin models under acid-free conditions with carbon-supported platinum catalysts. Chemical Communications, 47(44), 12209-12211.

Prochazkova, D., Zámostný, P., Bejblova, M., Červený, L., Čejka, J. 2007. Hydrodeoxygenation of aldehydes catalyzed by supported palladium catalysts. Applied Catalysis A: General, 332(1), 56-64.

Qin, Z., Shen, B., Yu, Z., Deng, F., Zhao, L., Zhou, S., Yuan, D., Gao, X., Wang, B., Zhao, H. 2013. A defect-based strategy for the preparation of mesoporous zeolite Y for high-performance catalytic cracking. Journal of Catalysis, 298, 102-111.

Scholze, B., Meier, D. 2001. Characterization of the water-insoluble fraction from pyrolysis oil (pyrolytic lignin). Part I. PY–GC/MS, FTIR, and functional groups. Journal of Analytical and Applied Pyrolysis, 60(1), 41-54.

Sheng, C., Azevedo, J. 2005. Estimating the higher heating value of biomass fuels from basic analysis data. biomass and bioenergy, 28(5), 499-507.

Sitthisa, S., Resasco, D.E. 2011. Hydrodeoxygenation of furfural over supported metal catalysts: A comparative study of Cu, Pd and Ni. Catalysis letters, 141(6), 784-791.

Tang, Z., Zhang, Y., Guo, Q. 2010. Catalytic hydrocracking of pyrolytic lignin to liquid fuel in supercritical ethanol. Industrial & Engineering Chemistry Research, 49(5), 2040-2046.

Torri, C., Reinikainen, M., Lindfors, C., Fabbri, D., Oasmaa, A., Kuoppala, E. 2010. Investigation on catalytic pyrolysis of pine sawdust: Catalyst screening by Py-GC-MIP-AED. Journal of Analytical and Applied Pyrolysis, 88(1), 7-13.

Wikberg, H., Liisa Maunu, S. 2004. Characterisation of thermally modified hard-and softwoods by ^{13}C CPMAS NMR. Carbohydrate Polymers, 58(4), 461-466.

Wildschut, J., Iqbal, M., Mahfud, F.H., Cabrera, I.M., Venderbosch, R.H., Heeres, H.J. 2010a. Insights in the hydrotreatment of fast pyrolysis oil using a ruthenium on carbon catalyst. Energy & Environmental Science, 3(7), 962-970.

Wildschut, J., Mahfud, F.H., Venderbosch, R.H., Heeres, H.J. 2009. Hydrotreatment of fast pyrolysis oil using heterogeneous noble-metal catalysts. Industrial & Engineering Chemistry Research, 48(23), 10324-10334.

Wildschut, J., Melián-Cabrera, I., Heeres, H. 2010b. Catalyst studies on the hydrotreatment of fast pyrolysis oil. Applied Catalysis B: Environmental, 99(1), 298-306.

Xu, W., Miller, S.J., Agrawal, P.K., Jones, C.W. 2012. Depolymerization and hydrodeoxygenation of switchgrass lignin with formic acid. ChemSusChem, 5(4), 667-675.

Zhang, Q., Chang, J., Wang, T., Xu, Y. 2007. Review of biomass pyrolysis oil properties and upgrading research. Energy Conversion and Management, 48(1), 87-92.

Zhao, C., He, J., Lemonidou, A.A., Li, X., Lercher, J.A. 2011. Aqueous-phase hydrodeoxygenation of bio-derived phenols to cycloalkanes. Journal of Catalysis, 280(1), 8-16.

Zhao, C., Kou, Y., Lemonidou, A.A., Li, X., Lercher, J.A. 2009. Highly Selective Catalytic Conversion of Phenolic Bio-Oil to Alkanes. Angewandte Chemie, 121(22), 4047-4050.

초 록

본 연구에서는 급속열분해를 통해 생성된 바이오오일의 수송용 연료화를 위한 개질 방법으로 수첨탈산소 공정을 수행하였다. 급속열분해를 통해 얻은 억새 바이오오일을 세 종류의 금속 촉매(Pd/C, Ru/C, Pt/C)를 이용하여 250-350℃, 30-60분 동안 30 bar 의 수소를 주입한 후 개질 공정을 진행하였다. 수첨탈산소 개질 공정 결과 가스와 탄 및 유기물로 이루어진 개질된 heavy oil 과 용매 및 물로 구성된 light oil 로 구분되는 액상의 오일이 생성되었다.

모든 heavy oil 의 물리적, 화학적 특성은 바이오오일과 비교하여 개선되었으며 촉매 종류 및 반응 조건에 따라 heavy oil 을 비롯한 생성물의 수율에 차이가 나타났다. 바이오오일의 수분 함량이 17.7%에서 0.1-0.8% (Pd/C), 0.5-8.2% (Ru/C), 0.5-4.0 (Pt/C)로 감소하였으며, 발열량은 17.3 MJ/kg 에서 22.8-25.9 MJ/kg (Pd/C), 23.3-26.1 MJ/kg (Ru/C), 20.7-27.8 MJ/kg (Pt/C)로 증가하였다. GC/MS 분석을 통해 확인된 약 33가지의 저분자량 화합물을 작용기에 따라 분류하였다. 이 중 불안정한 물질인 산(2-hydroxy-butanoic acid), 당(levoglucosan), 알코올(butaneidal) 및 알데하이드류(furfural)는 수첨탈산소 반응을 거치며 안정한 에스테르, 페놀류 물질로 다양하게 변화되었다. 또한 바이오오일의 구성성분 중 안정성을 저해하는 열분해 리그닌(22.4%)은 수첨탈산소 반응을 통해 바이오오일 대비 8.8-17.7% (Pd/C), 7.8-9.0% (Ru/C), 3.5-6.5% (Pt/C)로 감소하였다. 열분해 리그닌과

비교하여 heavy oil 내 페놀성 수산기와 메톡실기가 각각 감소하였다. Heavy oil 의 물성과 화학 조성의 변화 및 heavy oil 내 존재하는 페놀성중합체의 수율 및 특성 변화로부터 수첨탈산소 반응을 통해 바이오오일의 안정성이 향상된 것을 확인하였다.

수첨탈산소 촉매의 재사용 횟수가 증가함에 따라 각 촉매가 불활성화 되었으며 촉매 종류에 따라 각각 코크(coke) 침적(Pd/C, Ru/C, Pt/C), 황에 의한 피독(Ru/C, Pt/C) 및 금속과 메틸기의 결합으로 인한 활성점의 파괴(Pd/C) 등 다양한 불활성화 반응이 진행되었다.